

Lithium Metal Anodes: Advancing our Mechanistic Understanding of Cycling Phenomena in Liquid and Solid Electrolytes

Adrian J. Sanchez and Neil P. Dasgupta*



Cite This: *J. Am. Chem. Soc.* 2024, 146, 4282–4300



Read Online

ACCESS |

Metrics & More

Article Recommendations

ABSTRACT: Lithium metal anodes have the potential to be a disruptive technology for next-generation batteries with high energy densities, but their electrochemical performance is limited by a lack of fundamental understanding into the mechanistic origins that underpin their poor reversibility, morphological evolution (including dendrite growth), and interfacial instability. The goal of this perspective is to summarize the current state-of-the-art understanding of these phenomena, and highlight knowledge gaps where additional research is needed. The various stages of cycling are described sequentially, including nucleation, growth, open-circuit rest periods, and electrodissolution (stripping). A direct comparison of lessons learned from liquid and solid-state electrolyte systems is made throughout the discussion, providing cross-cutting insights between these research communities. Major themes of the discussion include electro-chemo-mechanical coupling, insights from *in situ/operando* analysis, and the interplay between experimental observations and computational modeling. Finally, a series of fundamental research questions are proposed to identify critical knowledge gaps and inform future research directions.

1. INTRODUCTION

The demand for electric vehicles is increasing worldwide.¹ This has been largely driven by improvements in Li-ion batteries, which have experienced a steady increase in energy density and cycle life over the past three decades.^{2–4} However, there remains great interest in developing rechargeable battery chemistries to address the electrification needs of more challenging sectors, including heavy-duty vehicles and electric aviation, which require a step increase in energy density.

One common feature of next-generation Li-battery chemistries that could theoretically enable higher energy densities is the replacement of the current graphite negative electrode (anode) with metallic Li. Li metal anodes exhibit both a high theoretical specific capacity (3680 mAh/g) and a highly negative potential (−3.05 V vs RHE), which can enable high energy densities in Li–S and Li–air batteries.⁵ For this reason, Li metal anodes have long been viewed as a “holy grail” of battery materials. However, to date, there are few examples of commercial Li-metal rechargeable batteries, as a result of several challenges, including:⁶

1. Poor reversibility/low Coulombic efficiency (CE)
2. Safety concerns (dendrites, thermal runaway)
3. Limited stability against both liquid and solid electrolytes
4. Supply chain concerns for metallic Li, resulting in inconsistent material properties
5. Manufacturing challenges

Over the past decade, there has been a renaissance in Li metal anode research, which is fueled by the demand for higher energy density. This renewed attention has led to improvements in certain cell performance metrics. For example, the development of new liquid electrolytes has enabled an increase

in CE to ~99.5%.⁷ This could facilitate a cycle life of ~50 if no excess Li is present in the anode, which can be increased to hundreds of cycles if excess Li inventory is provided at the negative electrode during cell assembly. Even higher values of CE have been reported for liquified gas electrolytes.^{8,9} In addition to these advances in electrolyte chemistry,^{10–18} 3-D architectures with “lithophilic” surface chemistries have resulted in improved control of nucleation and morphology.^{19–25} However, the reversible plating and stripping of Li metal is still significantly less efficient than cycling of intercalation-based Li-ion electrodes.²⁶

For the field to continue to progress, there is a need for additional fundamental research into the coupled (electro)-chemical, morphological, and mechanical evolution of Li metal anodes as they dynamically evolve during operation.^{27–40} Seven years ago, we wrote a perspective in *ACS Energy Letters* calling for more fundamental research into these coupled phenomena, and identifying critical knowledge gaps.⁴¹ Since then, some of these fundamental knowledge gaps have been addressed, while others remain unanswered, and several important new questions have arisen as the field has continued to develop.

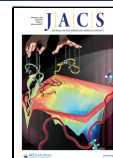
The overarching goal of this perspective is to provide an update on the current state-of-the-art in our scientific understanding of the fundamental mechanisms that guide Li

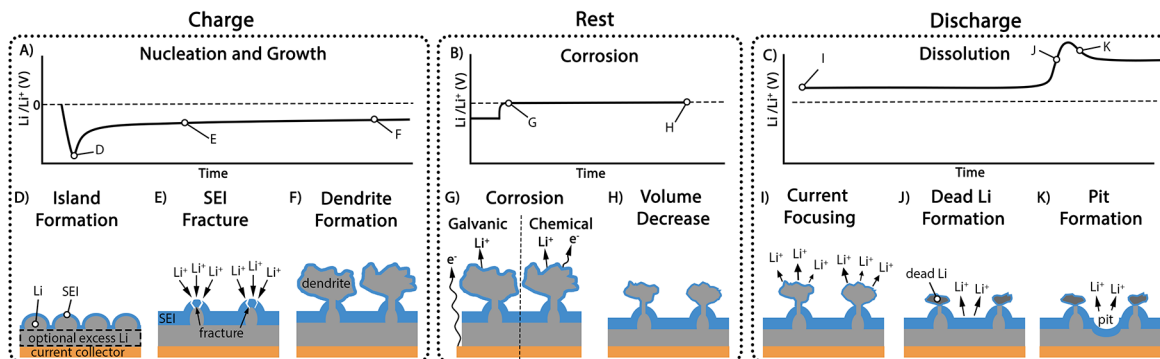
Received: May 31, 2023

Revised: January 10, 2024

Accepted: January 11, 2024

Published: February 9, 2024



Scheme 1. Dynamic Evolution of Li Cycling Separated into Three Phases^a

^a(a) Charging, (b) open-circuit resting, and (c) discharging. Illustrations of the morphological evolution are provided in panels (d–k).

plating, stripping, and corrosion. We note that this is not intended to be a comprehensive review article and point the reader toward several excellent reviews in recent years.^{7,42–53} We also do not emphasize applied engineering strategies or focus on device performance metrics, which remain the focus of the majority of the recent literature on Li metal anodes. Instead, we provide a reflection and perspective on the remaining knowledge gaps and scientific questions surrounding the fundamental properties and behavior of Li metal, with an emphasis on new questions that have arisen in recent years.

2. BACKGROUND AND DEFINITIONS

The logic of this perspective is organized around the major stages of cycling a Li metal anode, as illustrated in Scheme 1. We break down the cycling process into three general stages: charging (electrodeposition), resting (open-circuit), and discharging (electrodissolution/stripping). Scheme 1 shows a simplified representation of the morphological evolution of the anode during these stages, along with the corresponding anode voltage traces.

During the first charging step, electrodeposition initiates on an electrically conductive substrate. The flux of Li ions to the negative electrode surface is provided by oxidative half-reactions at the positive electrode (cathode). In the case of “anode-free” configurations, the initial substrate is composed of the current collector, while in cells with excess Li present at the anode, a thin metal foil is typically employed (Scheme 1D). The application of a charging current will result in concurrent nucleation of metallic Li and SEI formation, which can occur on both the surface of the current collector and on the surface of the freshly plated Li. During the initial nucleation stage, the anode potential decreases to values below the thermodynamic potential for Li plating (0 V vs Li/Li⁺), until a “nucleation peak” is typically observed in the voltage trace (Scheme 1A).^{54–56}

As charging continues, the voltage peak transitions into a plateau at a more positive potential as the plated surface area increases. As the initial nuclei grow larger in size, the surface morphology continues to evolve. In liquid electrolyte systems, this typically involves the formation of a variety of nonplanar morphologies, which can result in continuous mechanical fracture of the SEI on the plated Li surface.^{57–59} When SEI fracture occurs, a “fresh” Li metal surface is exposed to the electrolyte, promoting current focusing and new nucleation events (Scheme 1E). This can lead to the formation of 3-dimensional morphologies, including dendrites. In solid-state

systems, metallic filament growth can propagate across the cell and result in internal short-circuiting, which is associated with complex chemo-mechanical coupling. Further details on nucleation and growth are described in Sections 4 and 5 of the perspective.

At the end of charging, typically, a rest period occurs, where the cell is maintained under open-circuit conditions. The length of rest time, as well as environmental conditions (e.g., temperature, stack pressure), will influence the continual evolution of the Li metal anode during resting. Owing to the thermodynamic instability of Li against the vast majority of liquid and SSEs, continual SEI formation will occur. Relaxation of the electrode morphology may also occur through diffusion and/or creep processes. Furthermore, recent studies have highlighted the importance of corrosion processes during extended resting, which may be either galvanic or chemical in nature (Scheme 1G). These processes result in a decrease in the active Li inventory and calendar life of the battery. Further details on corrosion are described in Section 6.

During discharge, metallic Li is stripped from the anode. Depending on the physical and chemical properties of the anode (microstructure, morphology, SEI composition, etc.), the stripping process often results in inhomogeneous electrodissolution, which further drives the morphological evolution of the anode (Scheme 1I). Compared to plating, much less attention has been paid to the fundamental behavior of Li metal during stripping, resulting in larger knowledge gaps. In particular, one of the most detrimental, and still poorly understood process that can occur is the formation of “Dead Li”,^{28,38,56,60–64} which is defined as physically and/or electronically isolated Li metal domains that can accumulate on the surface and no longer contribute to the accessible inventory of the battery (Scheme 1J).

Inhomogeneous stripping can also result in surface pits (Scheme 1K), which experience their own set of nucleation and growth behaviors. While the specific voltage behavior during stripping can vary significantly depending on the existing plated Li morphology^{28,33,56,65–68} (including the presence/absence of excess Li), the general shape of the voltage trace for a system where pit formation occurs, is shown in Scheme 1c. An initial increase in cell polarization is observed as Dead Li is forming, which may be followed by a decrease in polarization as pits form on the remaining surface. These pits can promote current focusing and localized nucleation of plated Li in the following charging half-cycle.^{28,33} Inhomogeneous stripping and pit formation has been observed to occur

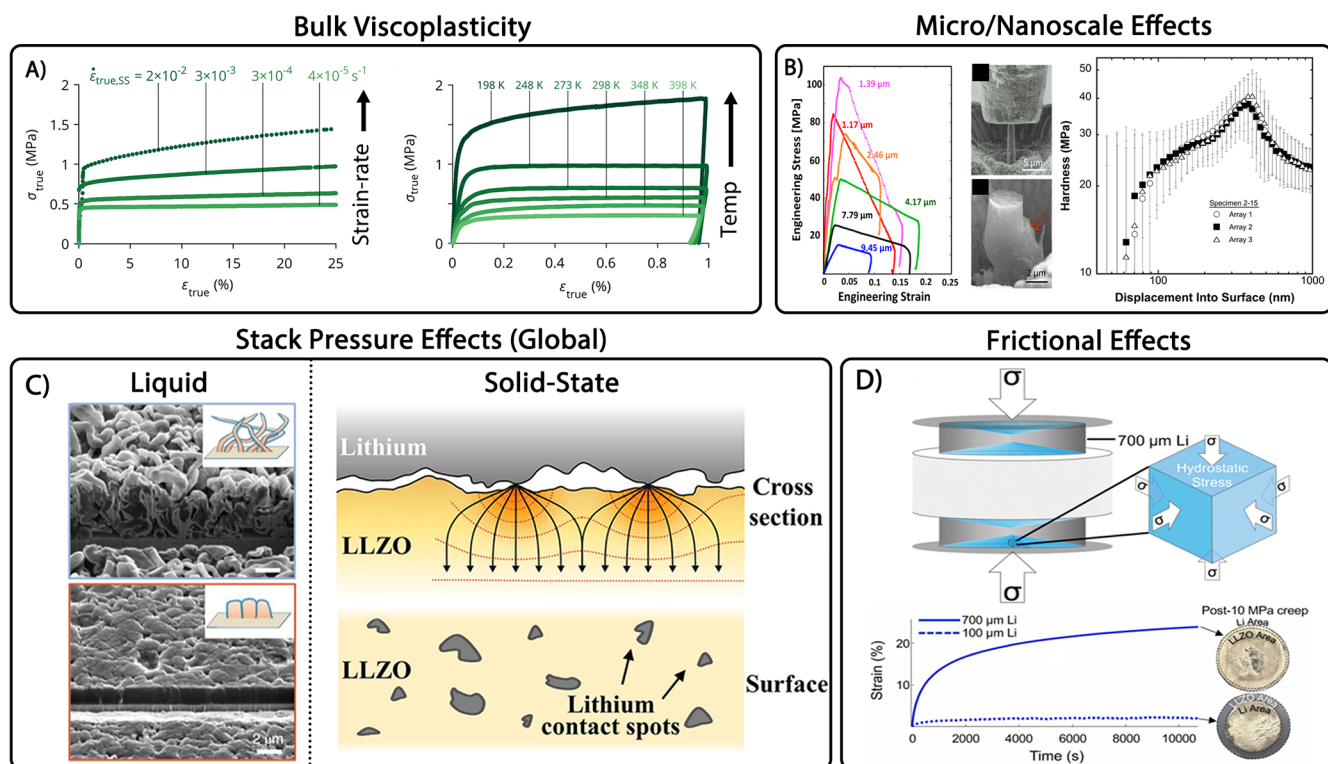


Figure 1. (A) Stress–strain curves for bulk Li foils, showing strain-rate and temperature dependences.⁶⁹ Reprinted with permission under a Creative Commons CC-BY 4.0 license from ref 69. Copyright 2019, Electrochemical Society. (B) Micro/nanoscale deformation tests, showing an increase in flow stress with decreasing size.^{70,71} Reprinted with permission from ref 70 (Copyright 2017, National Academy of Sciences) and ref 71 (Copyright 2018, Springer Nature). (C) Influence of stack pressure on Li metal anodes against liquid and SSEs.^{72,73} Reprinted with permission from ref 72 (Copyright 2021, Springer Nature) and ref 73 (Copyright 2019, American Chemical Society). (D) Frictional effects at Li/solid interfaces increase hydrostatic stress as the anode thickness decreases.⁷⁴ Reprinted with permission from ref 74. Copyright 2022, Elsevier.

in both liquid and SSE systems, where an important difference is that in liquids, the electrolyte can fill-in and wet the pit interior, while in solid-state systems, contact loss can occur in the pit region, resulting in a void. Further details on stripping behavior are discussed in Section 7.

We note that in Scheme 1A, we are only plotting the potential of the negative electrode (vs a hypothetical Li/Li⁺ reference electrode). In contrast, the voltage behavior of a full cell will also be influenced by the dynamically evolving positive-electrode potential. In general, to the extent that reference electrodes can be introduced into a 3-electrode cell geometry without significantly perturbing the system, a more complete and accurate understanding of the dynamic potential evolution of the negative electrode can be measured. However, recognizing that this is not always possible, this also highlights the importance of computational modeling of voltage changes, to avoid potential misinterpretations of the electrochemical signatures described above.

3. ELECTRO-CHEMO-MECHANICAL COUPLING

In addition to the chemical, morphological, and electrochemical phenomena described above, there has also been a growing recognition of the importance of coupled electro-chemo-mechanics. Here we provide a brief overview of recent progress in understanding the fundamental mechanical properties of Li, which are critical to guide the subsequent discussions.

The mechanical behavior of Li can be viewed through the lens of constitutive relationships, including elasticity, plasticity,

creep, and fracture. Recently, there have been several reports of the bulk mechanical response of Li,^{69,75} which were performed in chemically inert environments. The elastic modulus has been measured by pulsed echo techniques, and is approximately ~8 GPa.⁷⁵ Upon applying a mechanical load (in tension or compression), we immediately observe permanent deformation of Li, suggesting that the elastic limit of Li is very low (Figure 1a).⁶⁹ Furthermore, the stress–strain relationships of bulk Li are highly dependent on strain rate and temperature, as shown in Figure 1a.

Owing to the relatively low melting temperature of Li (~180 °C), creep can occur easily at or near room temperature, resulting in a viscoplastic response.⁶⁹ This has significant implications for the electro-chemo-mechanical coupling in Li-metal batteries, because strain rate couples directly with the ionic flux during plating and stripping (as described by Faraday's law), and is thus directly dependent on current density.⁶⁹ Furthermore, temperature fluctuations, which may be global (externally applied) or local (e.g., Joule heating) can change the mechanical response of Li significantly. Bulk deformation of Li exhibits power-law creep, which can be fitted to an Arrhenius curve to extract relevant activation energies. This highlights the importance of understanding the microstructure and presence of defects in Li, which can affect the flow of dislocations and Li vacancies during deformation.

In addition to these bulk observations, recent investigations have also studied the size-dependent mechanical response of Li. Examples include micropillar compression (Figure 1b)⁷⁰ and nanoindentation experiments (Figure 1c).^{71,76} The general

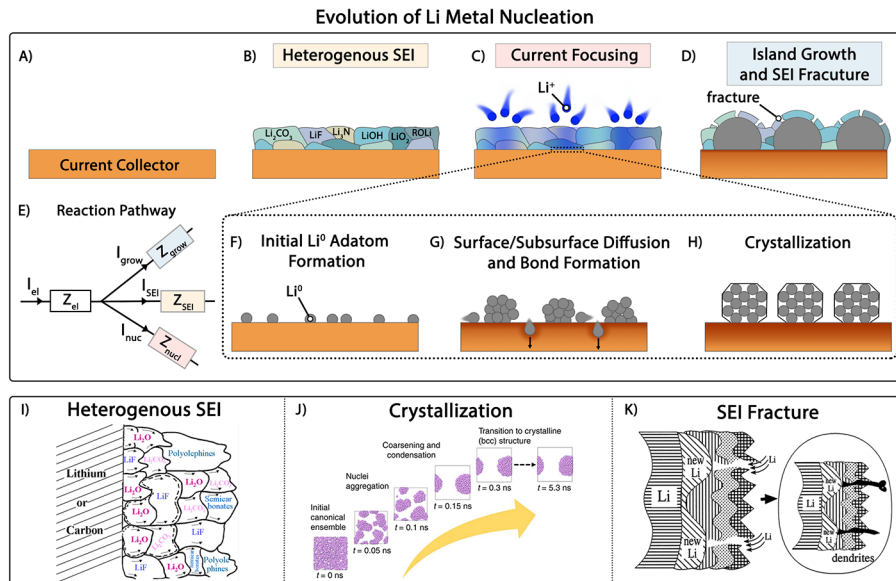


Figure 2. (A–D) Schematic of the stages of nucleation. (E) Equivalent circuit model of reaction pathways during plating. (F–H) High-magnification schematic of Li motion along the substrate surface, forming discrete nuclei. (I) Schematic of a heterogeneous SEI.⁸² Reprinted with permission under a Creative Commons CC-BY 4.0 license from ref 82. Copyright 2017, Electrochemical Society. (J) Evolution from amorphous Li clusters to crystalline Li nuclei.⁸³ Reproduced with permission from ref 83. Copyright 2020, Springer Nature. (K) Mechanical fracture of the SEI results in low impedance pathways for dendrite nucleation.⁵⁸ Reproduced with permission from ref 58. Copyright 2000, Elsevier.

observation has been that the viscoplastic (creep) response of Li also occurs at small length scales, although the overall flow stress required to deform Li at a specific strain rate increases. In other words, Li becomes more resistant to deformation at small length scales. While a detailed discussion of the chemical and physical origins of these size-dependent phenomena are beyond the scope of the current discussion, the readers are referred to several in-depth studies.^{70,71,76}

The consequences of this “hardening” of Li at small length scales could be significant, in particular when considering the early stages of nucleation, and final stages of stripping, where the Li domain size is at the nanoscale. In addition, size-dependent mechanics can play a role in the growth of filaments/dendrites, especially in SSE systems, where a mechanical crack-opening process is often ascribed to propagation.⁷⁷ Essentially, if Li is confined to a small space, it may become resistant to plastic flow, resulting in the accumulation of larger localized stresses within the crack opening.

Emergent chemo-mechanical phenomena also occur when an external “stack pressure” is applied, which is often in the range of kPa to MPa, depending on the cell type. For example, in liquid electrolyte systems, it has been observed that when the stack pressure is increased, a more dense plating morphology is observed,⁷² which corresponds with a higher CE upon cycling (Figure 1d). As will be discussed further in Section 7, mechanical compression of nonplanar Li morphologies can also significantly influence “Dead Li” formation, resulting in the formation of a compact and tortuous interphase upon extended cycling. In solid-state systems, stack pressure has also been observed to play a critical role in the cycling behavior.^{78–81} In particular, owing to the solid-solid nature of the Li/electrolyte interface, contact mechanics play an important role.

Finally, recent studies have also highlighted the importance that friction and adhesion play on the interfacial mechanics of

Li metal anodes. For example, it has been observed that the compressive force required to initiate viscoplastic flow increases significantly as the Li thickness decreases (Figure 1d).⁷⁴ This is attributed to frictional forces between the Li metal and the adjacent interfacial materials, resulting in the accumulation of hydrostatic stress within the Li metal. These frictional effects can play an important role in several aspects of Li metal anode dynamics, especially in solid-state systems, where the Li metal anode is in contact with the SSE and current collector. Friction can also play an important role in the mechanical deformation of nonplanar surface morphologies (e.g., extrusion out of surface flaws), which will influence the local stress distribution.

In the following sections, we discuss recent progress in understanding the fundamental mechanisms that guide each of the stages described in Scheme 1. Throughout the discussion, concepts from liquid and SSEs are woven together rather than treated as separate topics, to highlight cross-cutting learning opportunities. We start by describing heterogeneous nucleation during charging, followed by growth of plated Li. Next, we discuss the corrosion processes that occur during open-circuit rest periods. Finally, we describe the discharge (stripping) processes, emphasizing the current understanding of Dead Li formation and pit/void formation along the anode surface. We conclude with a perspective on the remaining scientific knowledge gaps and questions that need to be addressed to continue to build upon this foundational understanding.

4. NUCLEATION

As illustrated in Scheme 1, the cyclic electrodeposition and electrodissolution of metallic Li involves a series of stages, the first of which is nucleation. Immediately after cell assembly and before the first formation cycle, the negative electrode consists of a metallic phase in equilibrium with the electrolyte (Figure 2a). In the case of an “anode-free” configuration, the initial electrode is typically the current collector surface (which may

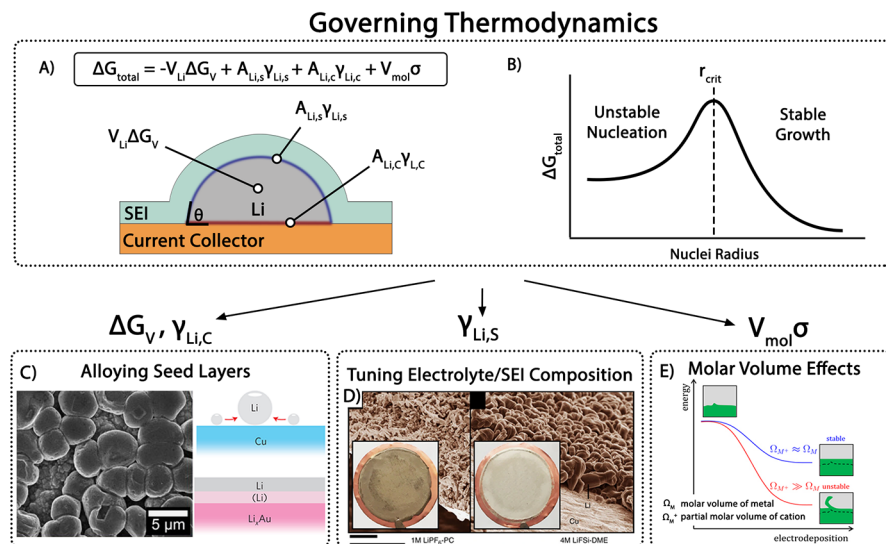


Figure 3. (A) The total Gibbs free energy change of a nucleating deposit on a substrate affects the contact angle. (B) Schematic of the critical radius during nucleation. This free energy balance can be affected through (C) introduction of alloying seed layers;^{99,100} adapted with permission from ref 99 (Copyright 2021, Electrochemical Society) and ref 100 (Copyright 2016, Springer Nature), (D) tuning electrolyte composition;¹⁴ reproduced with permission under a Creative Commons CC-BY 4.0 license from ref 14, Copyright 2015, Springer Nature, and (E) changes in molar volume due to mechanical strain;⁹⁸ reproduced with permission Reprinted with permission from ref 98, copyright 2020, Electrochemical Society.

be modified with a nucleation “seed layer”); when excess Li is present, the electrode surface is initially comprised of metallic Li. This initial interface may also be affected by the presence of an SEI layer, which spontaneously forms as soon as Li metal is brought into contact with the electrolyte. In the case of anode-free systems, the initial open-circuit potential of the electrode is typically positive vs Li/Li⁺, and an SEI layer forms on the surface of the current collector as the potential is decreased to more negative values during the initial formation cycle. Regardless of the initial configuration, the SEI that forms at the electrode/electrolyte interface is typically heterogeneous in nature (Figure 2b,i).^{84–88} The chemical, mechanical, and structural heterogeneity of this initial SEI plays a critical role in the subsequent nucleation phenomena.^{57–59}

As the electrode potential continually decreases during the first formation cycle, the SEI composition and structure can evolve. Once the electrode potential drops to values negative of 0 V vs Li/Li⁺, Li plating becomes thermodynamically accessible,^{54,55} but may still be kinetically limited. Eventually, when a sufficiently large overpotential is established at the negative electrode interface, Li⁺ ions will be reduced from the electrolyte, forming neutral Li⁰ adatoms (Figure 2f).

We note that the exact spatial locations where Li plating initiates will be strongly influenced by the heterogeneity of the SEI layer. This immediately brings up a level of complexity that is often overlooked in the plating literature: although the user typically defines a “global” current density (based on the projected surface area of the electrode), the “local” current density along the interfaces is spatially and temporally variant (Figure 2c). As a consequence, at the specific location(s) along the interface where nucleation is initiated, the local flux of Li ions will be significantly higher.³⁰ The details of the spatial and temporal evolution of the local current density along the interface are often unknown, representing a knowledge gap in our fundamental understanding of Li nucleation. While multiscale modeling can provide insights into this behavior, our ability to model nucleation depends on detailed knowledge

of the heterogeneous SEI, including the spatially varying kinetic rate constants and transport properties of the composite SEI,^{89–94} representing a complex problem to quantitatively understand.

Perhaps the most directly observable information about nucleation that we have is contained in the anode voltage trace, which often exhibits a nucleation “peak” when the predominant chemical reaction on the surface shifts from SEI formation to Li⁺ reduction (Scheme 1a). This represents an important concept, which we will refer to throughout the rest of this perspective, which is the *transition in reaction pathways* that occurs during galvanostatic plating and stripping reactions. This concept is illustrated schematically in Figure 2e. During galvanostatic charging, the total current will be distributed between various accessible reaction pathways, including SEI formation, nucleation of new Li deposits, and growth of existing deposits. This can be described by an equivalent circuit model, where each reaction pathway is represented as a parallel impedance element. The fractional distribution of the total current between these reaction pathways depends on the relative impedance of each, which varies spatially and temporally as the electrode potential, morphology, and surface chemistry evolve.⁵⁶ As a consequence, the Faradaic efficiency of the reductive current applied at the negative electrode during nucleation is time dependent, as the product yield shifts from SEI formation to plated Li. This highlights an important concept: Li metal nucleation is not a “static” event; it is dynamic in nature. We further note that these nucleation dynamics are dependent on the electrolyte; for example, localized concentration gradients in liquid electrolytes or microstructural defects in a SSE can further modulate the spatially varying kinetics of nucleation.

Once the reaction pathway transitions from SEI growth to the formation of Li⁰ adatoms along the surface, these adatoms start to diffuse. Depending on the local surface chemistry, they may react and form chemical bonds with surface functional groups or with the underlying current collector, or they may

remain physisorbed to the surface (Figure 2g). If the SEI is truly electronically insulating, then mass transport through the SEI phase occurs before a charge transfer event can occur, resulting in the presence of Li⁰ atoms at the substrate-SEI interface (Figure 2c). However, based on the observations that chemical and galvanic corrosion of Li occur during extended open-circuit rest periods (described in Section 6), it is clear that redox reactions can continue to occur despite the presence of an SEI layer, indicating the complexity of the coupled transport and reactivity of the interphase region.

The adatoms that do not react with the substrate can continue to diffuse along surface to form Li-Li bonds, resulting in clusters of metallic Li (Figure 2g). The surface diffusion of Li⁰ will be guided by the local energy landscape, which will be influenced by the presence of microstructural features (including grain boundaries), SEI species, etc., resulting in further spatial heterogeneity along the Li surface.

Thermodynamically, there is a driving force to form the BCC Li metal phase when a sufficient number of adatoms are present; however, this phase transformation will be affected by the surrounding substrate, SEI, and electrolyte interactions, and can be kinetically limited. In fact, recent studies have observed the initial formation of amorphous Li clusters during the early stages of nucleation, which evolve into the BCC Li phase upon continued growth (Figure 2j).⁸³ This raises a fundamental question: at what length (and time) scale does crystallization occur?

As the local coordination of Li evolves into the crystalline phase (Figure 2h), the resulting crystallographic texture of the film takes shape, which may not be representative of a random powder. This film texture may be further influenced by epitaxial interactions with the underlying surface. Overall, there remains a knowledge gap surrounding the nature of Li crystallization in the early stages, as well as the factors that control the resulting crystallite size, texture, and faceting.

To provide a framework to understand these phenomena, classical nucleation theory has been applied (Figure 3). In this framework, the stability of a local Li domain during the nucleation phase is determined by the change in Gibbs free energy (ΔG_{nucl}) as described in eq 1,^{95–97} where V_{Li} is the volume of the Li phase, $A_{\text{Li},s}$ and $\gamma_{\text{Li},s}$ are the interfacial area and energy between the deposit and the SEI, $A_{\text{Li},c}$ and $\gamma_{\text{Li},c}$ are the interfacial area and energy between the deposit and the underlying substrate, V_{mol} is the molar volume of Li, and σ is the hydrostatic component of the stress tensor in the Li deposit.⁹⁸

The transition from nucleation to stable growth occurs when the critical radius (r_{crit}) is reached (Figure 3B). This critical radius is determined by setting the derivative of eq 1 to zero. eq 2 shows the critical radius for a hemispherical deposit, where C1 is $(1/2 - 3/4 \cos \theta + 1/4 \cos^3 \theta)$, C2 is $1 - \cos \theta$, C3 $\sin^2 \theta$ and θ is the contact angle shown in Figure 3A.¹⁰¹

$$\nabla G_{\text{nucl}} = -V_{\text{Li}} \nabla G_v + A_{\text{Li},s} \gamma_{\text{Li},s} + A_{\text{Li},c} \gamma_{\text{Li},c} + V_{\text{mol}} \sigma \quad (1)$$

$$r_{\text{crit}} = -\frac{2C_2 \gamma_{\text{Li},s} + C_3 \gamma_{\text{Li},c}}{2C_1 G \nabla G_v} \quad (2)$$

By introducing the effects of substrate heterogeneity on nucleation, we can begin to incorporate some of the complexity that was illustrated schematically in Figure 2. For example, as shown in Figure 3c,^{99,100} the introduction of a chemically reactive substrate or an alloying seed layer has been

shown to have a profound impact on the morphology of Li metal deposits, resulting in larger and more compact deposits (Figure 3c).^{100,102–104} As a consequence of alloy formation, both the bulk ΔG_v and substrate interfacial energy terms will be affected. Changes to the substrate chemistry, including the presence of defects and microstructural features such as grain boundaries, will also impact the surface diffusion of adatoms (Figure 2g).¹⁰⁵ Epitaxial relationships with the substrate, which may induce lattice strain and defects such as dislocations, could also influence the $\gamma_{\text{Li},c}$ term.^{106–108} In addition to these substrate effects, $\gamma_{\text{Li},s}$ can be modulated by tuning electrolyte composition (Figure 3d).^{11,12,14–17}

Mechanical stresses during nucleation can arise both from residual strain at the nucleus/substrate interface and mechanical stack pressure, which will influence the free energy evolution by modulating the molar volume of Li (Figure 3e).⁹⁸ In SSE systems, these molar volume effects can be pronounced. For example, the electrochemical potential of Li nuclei in solid-state batteries (SSBs) has been observed to vary as a function of both externally applied stack pressure,¹⁰⁹ as well as “internal” stresses that arise in anode-free SSBs as individual nuclei grow in size.¹¹⁰

Collectively, the influences of the substrate, electrolyte, and strain on the morphological evolution and wetting behavior of Li metal have been used to categorize the “lithiophobicity” or “lithophilicity” of a system, as first introduced by Cui and co-workers.¹⁰⁰ It has generally been observed that a more lithophilic system is desirable to improve the density of Li electrodeposition throughout the nucleation and growth phases, which is particularly important when moving to high-surface area (3-D) electrode geometries. However, to date, most of the discussion on lithiophobicity has been largely qualitative in nature, as reported through ex situ photographs or optical/electron microscopy images after Li plating. This represents an opportunity for more quantitative studies in the future, which can leverage the framework of surface science to understand wetting behavior. For example, quantitative contact angle measurements have been reported using by performing sessile drop tests with molten Li droplets, which have been rationalized by first-principles calculations of the work of adhesion between Li and a SSE.¹¹¹ Additionally, in situ/operando analysis of Li plating have been used to provide a valuable insight into the dynamic nature of Li wettability across length and time scales.^{27,30,37,38,99,112} In the future, there is a strong motivation to continue to develop advanced experimental and computational methods to continue to understand the complex nature of Li wetting during nucleation.^{113,114}

The equilibrium conditions depicted in Figure 3 will be further perturbed when a nonzero current is applied. For an electrodeposition process, the change in the Gibbs free energy of the system is described in eq 3, where z is the valency of the ion, e is the elementary electric charge constant, V_{mol} is molar volume, and η is overpotential.^{95,96}

$$\nabla G_v = -\frac{ze\eta}{V_{\text{mol}}} \quad (3)$$

By combining eqs 2 and 3, an inverse relationship between overpotential and critical radius can be seen. The overpotential can be further related to the current density through the Butler–Volmer eq (eq 4) where i is current, K° is the standard heterogeneous rate constant, T is temperature, α is the charge-transfer symmetry coefficient, R is the gas constant, η is overpotential, F is Faraday’s constant, C_{Li} is the surface

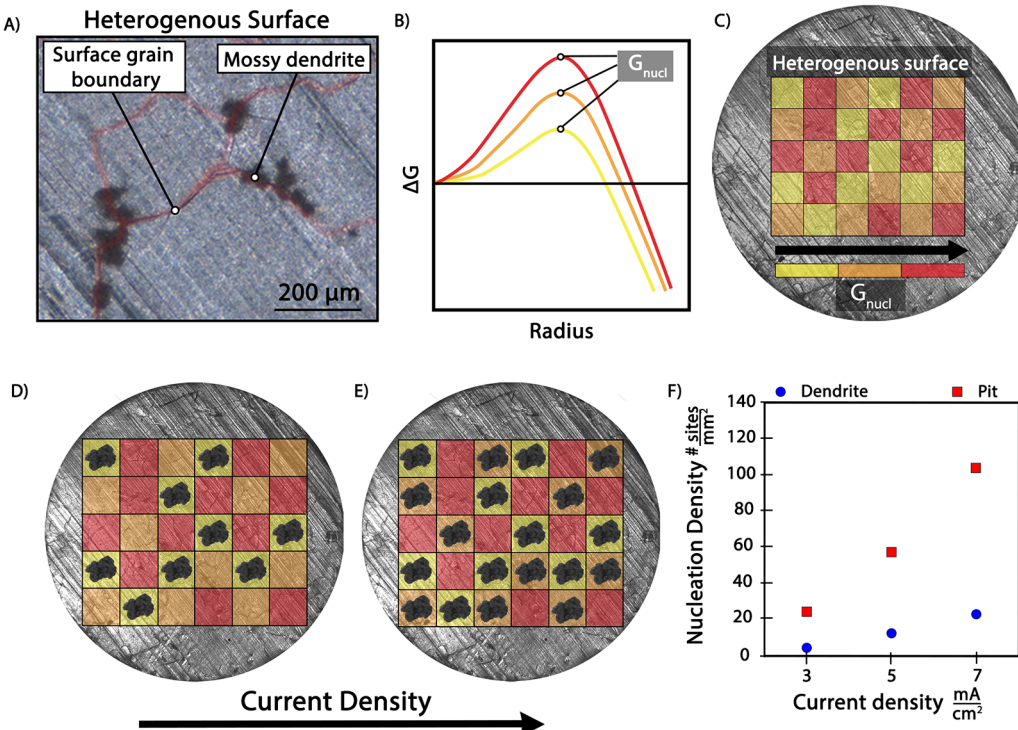


Figure 4. (A) Preferential nucleation at surface grain boundaries on Li metal. (B,C) Schematic of a spatially varying nucleation barrier and (D,E) increasing nucleation density as a function of current density. (F) Experimentally observed nucleation density of dendrites and pits vs current density.²⁸ Adapted with permission from ref 28. Copyright 2020, American Chemical Society.

concentration of Li, and C_{Li}^+ is the local electrolyte concentration of Li.^{28,56}

$$i = FK^o \left\{ c_{\text{Li}} \exp\left(\frac{(1-\alpha)F}{RT} \eta\right) - c_{\text{Li}}^+ \exp\left(-\frac{\alpha F}{RT} \eta\right) \right\} \quad (4)$$

These relationships have been quantitatively explored in anode-free cells, where higher current densities have been shown to promote smaller nuclei and larger nucleation areal densities.^{54,55} Biswal et al. expanded upon this model to incorporate the influence of mass transport through the electrolyte and SEI phases on nucleation, showing that higher diffusivity values and a higher surface energy promote more uniform deposition and smaller nuclei.⁵⁵

The framework above can be further modified to incorporate spatial variations in the local activation barrier for nucleation along the surface, which naturally arise from chemical and/or structural heterogeneity along the substrate.^{28,84–86,88,115} Figure 4b,c illustrates these variations in the local energy landscape along an electrode surface,²⁸ where the grid colors represent the magnitude of the local nucleation barrier (G_{nucl}).²⁸ As the global current density increases, the total electrode overpotential (driving force for nucleation) increases, resulting in higher nucleation density as more sites become accessible (eq 4). This influence of surface heterogeneity on the local nucleation density has been experimentally observed for both dendrites (during plating) and pits (during stripping, Figure 4f).²⁸ For example, variations in the electrode microstructure, such as surface grain boundaries (Figure 4A), surface topology,^{116,117} and surface chemistry have been observed to cause preferential nucleation.¹¹⁵ The heterogeneous nature of Li nucleation will influence the subsequent growth, stripping, and corrosion processes (described below),

illustrating the importance of additional fundamental research into the factors that affect nucleation.

5. LI METAL GROWTH

Once the dimensions of the Li nuclei exceed the critical radius (Figure 3b), the predominant reaction pathway transitions from nucleation to growth (Figure 2e). Recent studies have demonstrated several factors that can influence the morphology of Li during the growth stage (Figure 5).^{38,39,72,83,118–137} First, we note that the growth behavior is directly affected by the nature of nucleation, and thus these stages cannot be fully decoupled. For example, the increased nucleation densities observed at higher current densities will affect the subsequent aggregation of Li during the growth stage. Additionally, the crystallographic texture of Li nuclei, which is affected by both substrate interactions and the transition from amorphous to crystalline Li deposits, will affect the subsequent growth morphology.⁸³ This crystallographic texture has been observed to continue to evolve during extended plating, which can result in preferential exposure of specific facets to the electrolyte.¹³²

As the reaction pathway progresses from the nano- to microscopic length scales, various morphologies have been observed. Examples of commonly reported Li morphologies in liquid electrolytes include columnar, hemispherical, needle-like, mossy, and fractal growth.⁴¹ Distinguishing each morphology is critical, both to understand the fundamental mechanisms of Li growth and to identify the relationships between growth morphology and performance. This is further complicated by experimental observations that the growth morphology can evolve throughout deposition.

A specific growth morphology at a given point in plating can be thought of as a distinct reaction pathway (analogous to Figure 2e), and transitions can occur between these pathways.

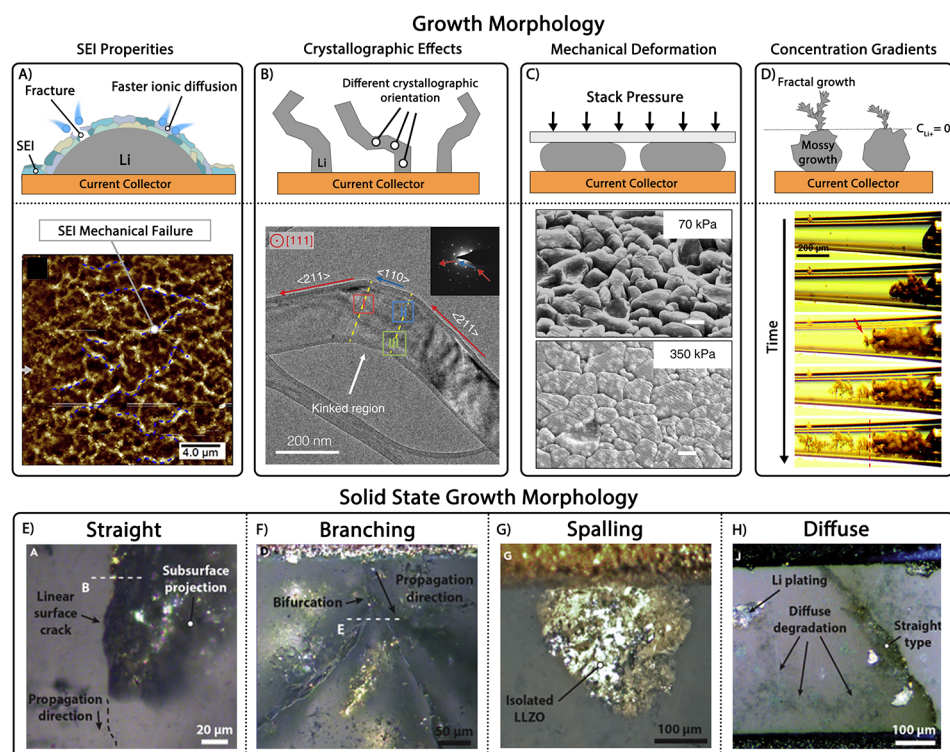


Figure 5. Factors influencing Li growth morphology. (A) SEI fracture can result in local “hot spots”.⁵⁹ Reproduced with permission from ref 59. Copyright 2020, Elsevier. (B) The faceting of Li deposits can result in anisotropic growth, including kinks.¹¹⁸ Reproduced with permission from ref 118. Copyright 2017, American Association for the Advancement of Science. (C) Stack pressure can result in a flattened growth morphology.⁷² Reproduced with permission from ref 72. Copyright 2021, Springer Nature. (D) Mass transport limitations at high current densities can drive dendritic growth.³⁹ Reprinted with permission under a Creative Commons CC-BY-NC 3.0 license from ref 39. Copyright 2016, Royal Society of Chemistry. (E–H) Various growth morphologies observed for Li filaments in ceramic SSEs.⁴⁰ Reproduced with permission from ref 40. Copyright 2020, CellPress.

For example, fractal growth has been observed to initiate after the initial deposition of mossy Li, which occurs when the limiting current density is reached (Figure 5d).³⁹ Overall, several factors can impact the dynamic deposition morphology, including electrolyte composition, current density, stack pressure/mechanical stresses, current collector architecture, and temperature.¹³⁸

A prominent factor impacting deposition morphology is the SEI. Recently, cryoelectron microscopy has revealed the detailed structure of the SEI on Li metal, which can vary depending on the electrolyte (e.g., mosaic vs layered).¹³⁹ The inhomogeneous SEI will result in spatially varying kinetics along the Li surface, resulting in current focusing during plating and stripping. In situ TEM has shown that mechanical stresses in the SEI can drive the formation of whisker-like growth. Following SEI fracture (Figure 5a),⁵⁹ the deposit rapidly grows outward from the anode surface. The rapid expansion creates a branch of whisker-like growth. Ultimately, repeated fracturing of the SEI and branching events can manifest as mossy Li, although the detailed evolution of mossy Li formation remains a complex problem that is difficult to quantitatively describe in current models.

The SEI composition on Li can vary significantly as a function of electrolyte composition.^{7,140,141} Carbonate electrolytes developed for Li-ion batteries promote the formation of sparse, mossy dendrites that display poor reversibility. In contrast, ether-based electrolytes can promote the formation of hemispherical deposits that achieve higher CE.¹⁴ The solvents of these electrolytes produce a variety of SEI chemistries. For

example, the common ethylene carbonate solvent leads to the formation of $(\text{CH}_2\text{OCO}_2\text{Li})_2$, while 1,2-dimethoxyethane promotes CH_3OLi .¹⁴² Electrolyte additives such as LiNO_3 can also alter the structure of the deposited Li.^{12,15,133} Another recent strategy to promote high CE is the development of “localized high-concentration” electrolytes, where a dual solvent system is used to decouple the coordination environment of the solvated Li^+ ion from the overall solution molarity. While a more detailed discussion of electrolyte chemistry is beyond the scope of this perspective, we refer the reader to recent reviews that describe the progress in electrolyte chemistry.⁷

Another strategy to modify the interfacial chemistry is the incorporation of “artificial SEI” layers. While there has been recent progress in the use of methods such as atomic layer deposition (ALD),^{143–148} developing coatings that can capture and control the full complexity of SEI behavior remains a challenge. For example, in SSBs, the use of Al_2O_3 interlayers (a standard artificial SEI/CEI layer used with intercalation materials) was observed to be insufficient to prevent decomposition of sulfide SSEs.¹⁴⁹ This was attributed to mechanical fracture of the brittle ceramic interlayer, highlighting the importance of fracture toughness when designing robust interlayers for Li metal anodes, including organic/inorganic interlayers.¹⁵⁰

Despite these advances, there are numerous remaining questions about SEI formation and its role in Li growth. Prominent questions include: (1) which SEI properties are most important to performance, and (2) what is the ideal SEI

structure and composition? The current understanding of SEI formation needs to be built upon to answer these questions. For example, in continuum-scale models, the SEI on Li is often treated as a single surface layer with effective transport and kinetic properties that are meant to represent its average behavior.¹⁵¹ However, as described above, the SEI is a composite material with spatial and temporal variations in its local structure, composition, kinetics, and mechanical properties, which should be taken into account in future modeling efforts.

Another factor impacting the growth morphology is the crystallographic orientation of deposited Li. During the initial stages of whisker-like growth, the orientation of the plated can vary, producing kinks (Figure 5b).¹¹⁸ As described above, this crystallographic faceting can evolve as the plated Li thickness increases, further influencing electrode reversibility.¹³² The crystallographic orientation of plated Li is a variable that can potentially be tuned to improve performance. However, the factors that control the crystallographic orientation of deposited Li are not fully understood.

To address this knowledge gap, new methodologies to control the orientation of plated Li in both liquid and solid electrolytes are needed. Toward this goal, the Li metal anode community can leverage knowledge from the nanomaterial synthesis field, including use of catalysts, electrolyte additives that selectively bind to specific facets, controlling epitaxial relationships, and more. In situations where excess Li is incorporated at the negative electrode, there is also a need for advances in metallurgical processing to control the crystallographic texture and surface chemistry of Li. For example, mechanical rolling of Li foils results in an anisotropic texture, which has been shown to influence both the plating and stripping morphology.^{28,33,65} However, current variations in the supply chain of thin Li foils can be significant, varying from vendor-to-vendor and over time. Therefore, improved control of Li film structure and composition is needed, both to enable systematic studies and also to enable future manufacturing of Li-metal batteries.

Other factors that impact the deposition morphology include surface diffusivity and surface energy. These properties have been studied extensively in other metal anodes, and this knowledge can be leveraged toward Li metal anodes.^{152–154} Overall, the equilibrium shape of a metal deposit is dictated by the surface energy, which can be visualized in a Wulff plot. However, the rate of surface diffusion can alter the growth morphology. For example, Li metal anodes have been compared to Mg anodes, where dendrite formation is not as prominent.^{155,156} Mg anodes display a higher surface diffusion coefficient, which is posited to mitigate dendrite formation.^{155–157}

Finally, mechanical stress and strain will also have a significant impact on the plated Li morphology.^{125,127,130} If a stack pressure is applied that exceeds the yield/flow stress of Li, then viscoplastic deformation will occur. This results in a “flattened” morphology (Figure 5c),⁷² where vertical growth is physically constrained.⁶⁹ The extent of this mechanical deformation will depend on the strain-rate and temperature of Li, as described in Section 3.

We further note that all of the above discussion, which focused largely on liquid electrolyte systems, will also be relevant for SSBs. However, the relative importance of the factors that control growth in solid-state systems may vary significantly. Analogous to liquid systems, a range of different

Li growth morphologies has been observed with SSEs. For example, in Figure 5e–h,⁴⁰ four distinct growth morphologies of Li filaments were observed using operando optical microscopy.⁴⁰

Mechanics play a particularly important role in determining the growth morphology within SSEs. For example, mechanical extrusion of Li from surface flaws has been proposed to be a limiting factor in determining the critical current density (CCD) for plating.⁷⁷ The CCD has been shown to increase exponentially with temperature, which will be influenced by the temperature dependence of both diffusion and viscoplasticity.¹⁵⁸ There is also increasing attention being paid to the roles of friction and contact mechanics in solid-state systems, which are unique to solid–solid interfaces, as discussed in Section 3.^{74,159} The incorporation of carbon/Ag interlayers in anode-free SSBs has been shown to promote Li growth at the back interface with the current collector, suppressing Li plating at the SE interface.¹⁶⁰ In general, compared to liquid systems, there is significantly less fundamental knowledge about the factors that govern Li growth in SE systems, representing an area of rapid scientific growth. For further details on these mechanisms, the reader is referred to recent review articles.^{161–166}

6. LI CORROSION

Throughout the cycle life of a Li metal anode, there will be several open-circuit rest periods, which may vary in their duration based on the duty cycle of the battery. The first rest period occurs at the end of the first charging cycle, which will be the focus of our discussion here. However, we note that the dynamic phenomena that occur during open-circuit rests can vary significantly, depending on the state-of-charge and state-of-health of the battery, as well as environmental factors including temperature and pressure.

One of the most important processes that occurs during open-circuit resting is the corrosion of metallic Li, of which there are two forms. *Galvanic corrosion* describes the process wherein the Li and current collector act as a corrosion couple (Figure 6a), resulting in a loss of Li inventory. In this process, Li is oxidized at the electrolyte interface, while the corresponding reduction reaction occurs at the interface between the current collector and electrolyte. This requires exposure of both the Li and current collector (e.g., copper)

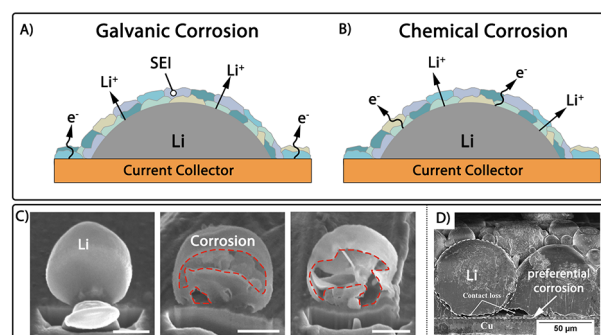


Figure 6. Schematic illustration of (A) galvanic corrosion and (B) chemical corrosion. (C) SEM images of galvanic corrosion.¹⁶⁷ Reproduced with permission from ref 167. Copyright 2019, Springer Nature. (D) SEM images of the corrosion of a powdered Li electrode.¹⁶⁸ Reproduced with permission under a Creative Commons CC-BY 4.0 license from ref 168. Copyright 2020, Wiley.

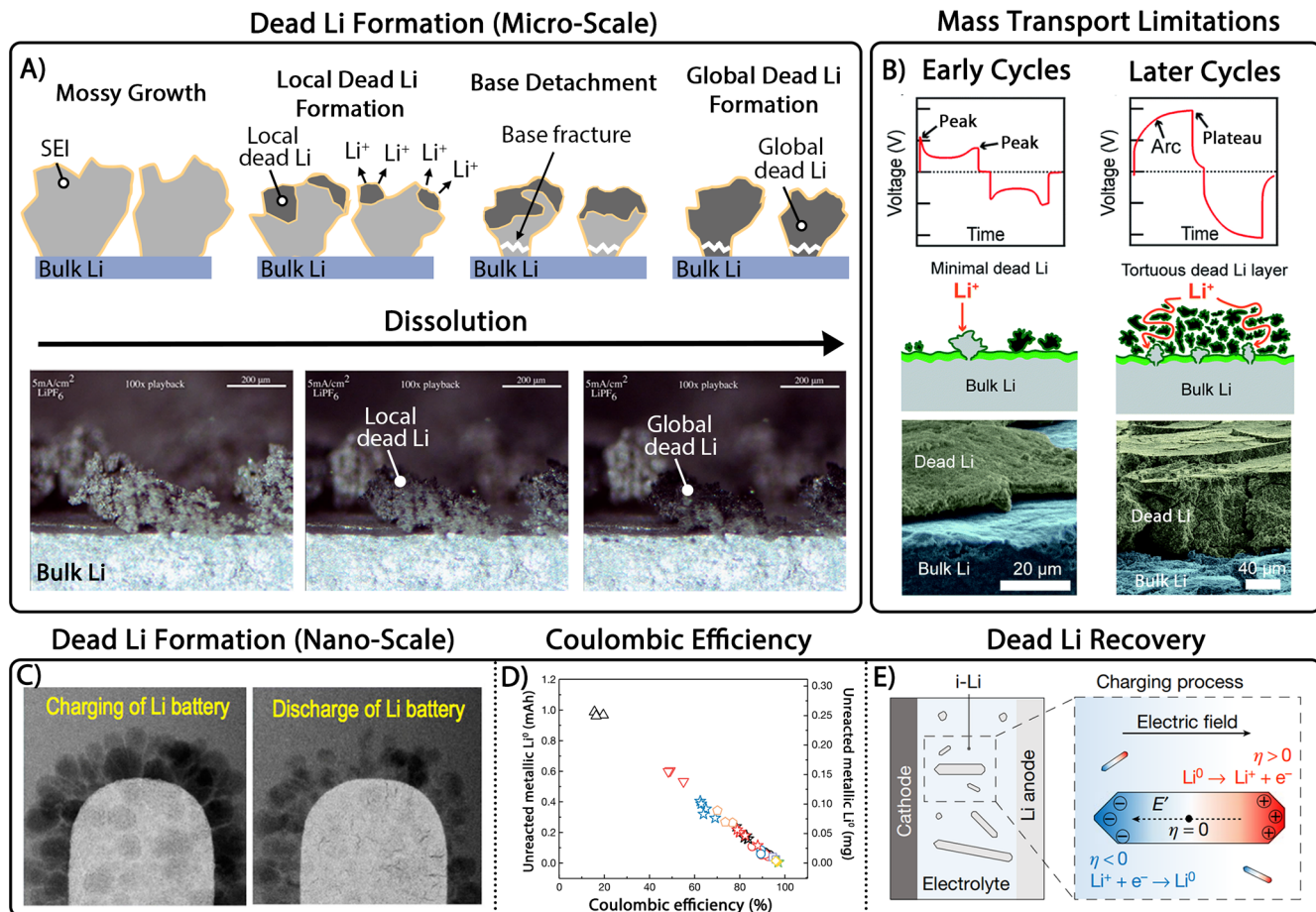


Figure 7. (A) Schematic and optical images of Dead Li formation.⁵⁶ Reprinted with permission from ref 56. Copyright 2016, American Chemical Society. (B) Mass transport limitations caused by accumulated Dead Li at anode surface.⁶³ Reproduced with permission from ref 63. Copyright 2017, Royal Society of Chemistry. (C) Operando electrochemical (S)TEM images of Li metal cycling.¹⁷² Reproduced with permission from ref 172. Copyright 2015, American Chemical Society. (D) Relationship between CE and Dead Li shown by TGC.⁶⁴ Reproduced with permission from ref 64. Copyright 2019, Springer Nature. (E) Schematic of electric field distribution along a Li⁺.⁶¹ Reproduced with permission from ref 61. Copyright 2021, Springer Nature.

surface to the electrolyte. Ex situ SEM observations have been performed on Li deposits after various rest periods in a liquid electrolyte, and volumetric shrinkage of plated Li was observed, resulting in Kirkendall-type void formation.¹⁶⁷ In the future, further studies are needed to reveal the detailed chemical mechanisms and reaction products formed during galvanic corrosion.

The other relevant form of corrosion is *chemical corrosion*, where both the electron and Li oxidation charge transfer events occur at the Li/electrolyte interface (Figure 6b). Chemical corrosion can also serve as a pathway for significant capacity losses. Ex situ SEM and TEM observations have shown that 2–3% of the total charge capacity can be lost within 24 h while a Li metal battery is at rest.¹⁶⁹ The relative rate of corrosion will be strongly dependent on the electrolyte composition, but in general, there is a growing consensus that the calendar life of Li metal anodes may pose a significant challenge. This is particularly important for EV applications, where the battery pack is largely held under open-circuit conditions.

Recent studies have elucidated several factors that impact the corrosion rate.⁶⁰ Using powder-based Li metal electrodes, the relative rate of galvanic corrosion was shown to be spatially variant.¹⁶⁸ Corrosion occurred more rapidly near the Li/current collector junction. This can exacerbate Dead Li

formation (described in Section 7), by accelerating local detachment at the current collector interface. Furthermore, the stack pressure,⁷² composition of the current collector and electrolyte,^{170,171} and protective coatings have been demonstrated to control the rate of corrosion.^{172,167} These influence the exposed surface area and kinetics of corrosion. Overall, fundamental studies of corrosion are relatively new to the Li metal anode community. This highlights an aspect of battery degradation that is crucial in commercial applications: calendar life, which can benefit from the existing knowledge base for Li-ion batteries.

7. LI ELECTRODISSOLUTION (STRIPPING)

The final stage of Li metal cycling shown in Scheme 1 is electrodissolution (stripping). Compared to plating, the stripping behavior of Li metal is less well studied. Despite this fact, stripping is a critical process can influence capacity loss and the morphological evolution during subsequent charging. Several reaction pathways exist during electrodissolution, which are detailed below.

At the beginning of a stripping half-cycle, Li is predominantly removed from the freshly deposited Li from the previous charging step.^{28,56} This reaction pathway can drive capacity losses through the electrical and/or physical isolation

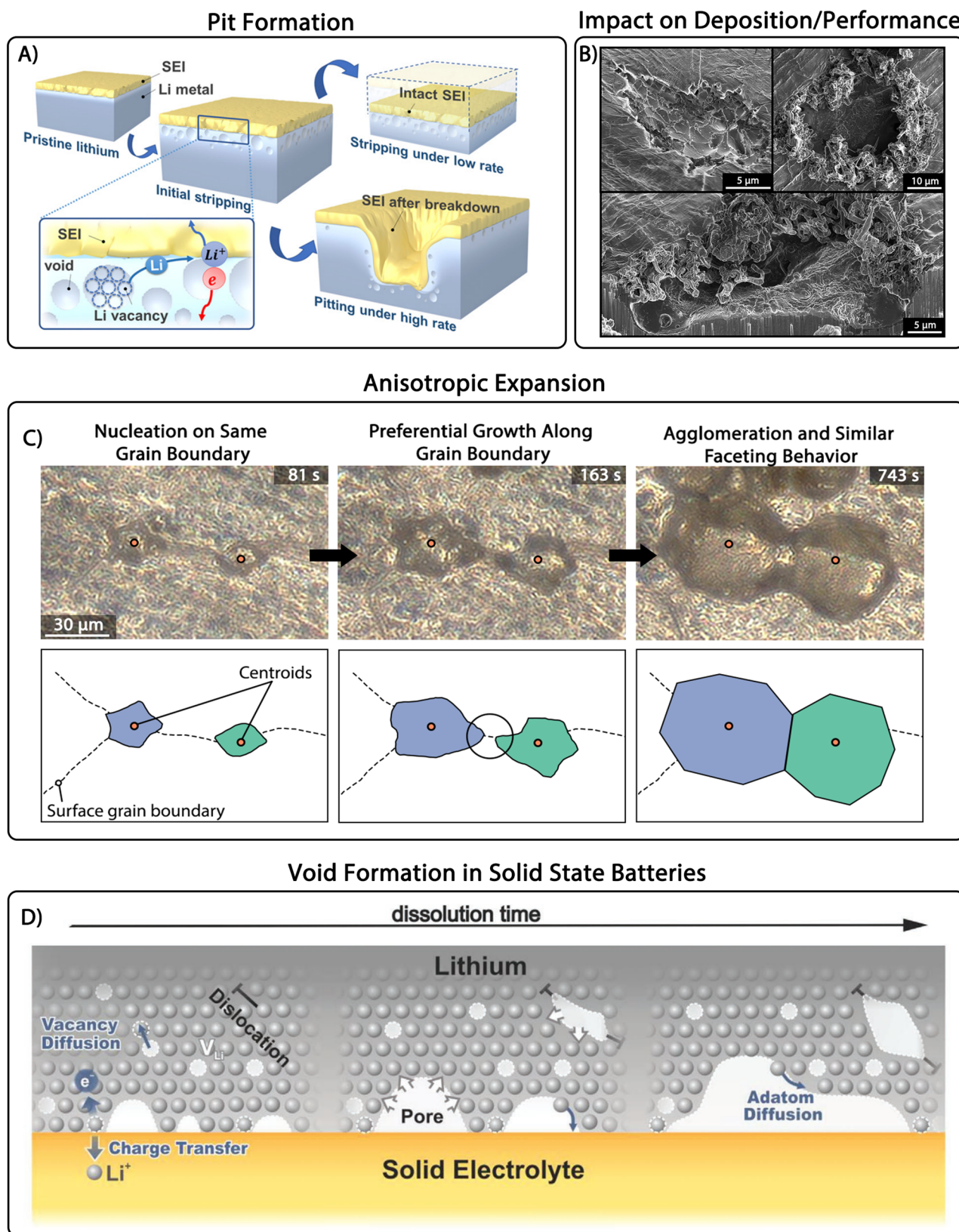


Figure 8. (A) Schematic of void accumulation, pit formation, and SEI collapse.⁶⁵ Reproduced with permission from ref 65. Copyright 2018, National Academy of Sciences. (B) SEM images of dendrite nucleation at pit edge.²⁸ Reproduced with permission from ref 28. Copyright 2020, American Chemical Society. (C) Optical images of pit expansion and edge faceting.³³ Reproduced with permission from ref 33. Copyright 2021, Royal Society of Chemistry. (D) Schematic of void formation in SSBs.⁹¹ Reproduced with permission under a Creative Commons CC-BY 4.0 license from ref 91. Copyright 2020, Wiley.

of active Li, which is often referred to as “Dead Li”, or “isolated Li” (Figure 7).^{60–64} While many factors can influence the capacity loss from Dead Li formation, a prominent factor is the deposited Li morphology. Recent cryo-FIB and TGC experiments have demonstrated that whisker-like and tortuous morphologies promote Dead Li formation.⁶⁴ It has been posited that these morphologies promote current focusing, which can lead to the local depletion of Li. Eventually, the SEI will collapse, which can generate isolated segments of Li (Figure 7a). In situ TEM measurements have shown that such current focusing can be driven by variations in the thickness of the SEI.³⁸ Therefore, preferential stripping occurs in specific locations, which isolates the Li from the bulk electrode. In general, the same factors that impact the growth of Li metal (described in Section 5) will heavily impact Dead Li formation.

Dead Li formation has the potential to be a bottleneck for the commercialization of rechargeable Li-metal batteries. However, to date, a full mechanistic understanding of how Dead Li forms is lacking. Operando video microscopy has elucidated the dynamic morphological evolution of mossy deposits during stripping (Figure 7a).⁵⁶ Initially, the top of the deposits develop a darkened texture, which is indicative of local Dead Li formation. As stripping continues, the local formation of Dead Li propagates from the top toward the base of the deposits. Once base detachment occurs, all remaining Li becomes isolated and Dead Li forms globally. However, even if the stripping process is terminated before the end of discharge, the formation of local Dead Li results in capacity loss.

During extended cycling of a Li metal anode, Dead Li from each cycle can accumulate on the surface (Figure 7b).⁶³ This results in the formation of a “compact interphase”, which grows thicker with increasing cycle numbers. As a consequence, mass transport of ions within the liquid electrolyte phase can become more limited, resulting in a depletion of the Li concentration at the active interface, which is buried beneath the Dead Li layer. This results in a change in the electrochemical signature during stripping from a peaking to arcing shape, which has been described by computational modeling of interfacial kinetics.^{63,151} It is important to note that many studies simply call this compact interphase the “SEI region”; however, the interphase is composed of a mixture of Dead Li and SEI. As a consequence of these mass transport limitations, the accessible rate of Li metal full cells at a given C-rate is often observed, which results in “power fade” of the cell.

A common methodology to quantify CE is to perform an initial formation cycle with a larger Li reservoir, and subsequently cycle a fraction of that charge capacity.¹⁷³ After shuttling the partial capacity for several cycles, Li is fully stripped to quantify the loss in Li inventory. The amount of partial charge that is cycled will dictate the extent of local vs global Dead Li formation, which impacts the Coulombic inefficiency, although a detailed mechanistic understanding of these depth-of-discharge effects is lacking. This has important implications for industrial applications, where the duty cycle of the electrode may vary dramatically.

Recently, titration gas chromatography (TGC) has been introduced as a powerful technique for quantifying the relative contributions of Dead Li and SEI formation to CE.⁶⁴ In this method, by dissolving a Li metal anode in water and measuring the gaseous byproducts, quantitative analysis can be performed (Figure 7d).⁶⁴ These studies have revealed the importance of electrolyte composition on both of these Li loss pathways, and

TGC is now becoming a more standard process for quantifying Li losses.

Another recent discovery that has impacted our understanding Dead Li dynamics has been the observation that under certain conditions, inactive Li can be recovered.⁶¹ For example, it has been observed that under high-current-density discharge conditions, Li migration can occur toward the current collector, which is driven by a gradient in electrochemical potential between the two ends of the isolated Li (Figure 7e).⁶¹ This can sometimes result in reattachment of Dead Li, resulting in partial recovery of the Li inventory. This recovery of Dead Li through high-current-density discharge in liquid electrolytes is in contrast to the “healing” of dendrites in solid-state systems when small current densities are implemented.¹⁷⁴ In the future, further fundamental studies on the detailed mechanism of this reattachment process would be impactful. For example, reattachment and recovery of Dead Li must require re-establishment of electrical contact between the Dead Li and current collector, which must coincide with changes (such as local fracture) to the electronically insulating SEI surrounding the Dead Li.

After global Dead Li formation, a transition in reaction pathways occurs, where additional stripping must occur from the surrounding “bulk” Li reservoir. In the case of anode-free cells, this may result in the immediate polarization of the negative electrode potential if the Li capacity is fully exhausted. However, if excess Li is present, stripping can proceed. Owing to the heterogeneous nature of the SEI and Li growth microstructure (Section 5), stripping does not occur uniformly, which can result in surface pitting.^{28,33,65,66,68,175} At an atomistic level, Li vacancies generated during stripping agglomerate into volumetric voids. The accumulation of these voids at the surface produces a crater-like morphology. Eventually, as these voids grow sufficiently large, the SEI mechanically collapses into the pit, which is driven by the pressure gradient between the electrolyte and subsurface void region (Figure 8a).⁶⁵

Compared to plating behavior, pit formation is largely overlooked in the literature, yet pits have been observed to directly impact the subsequent plating cycles and extended cycling behavior. For example, ex situ SEM and operando optical microscopy analysis have shown that the perimeter of a pit can serve as a preferential hot spot for dendrite nucleation during the subsequent plating cycle (Figure 8b).²⁸ Furthermore, the reversibility of Li plating and stripping is influenced by the size of the pits formed in early cycles.

These observations highlight two key points: (1) there is a “memory” effect when cycling Li metal, where the stripping behavior can strongly influence the reversibility and morphology of the subsequent plating cycles (this is true for both liquid and SSE systems); and (2) Dead Li formation is strongly influenced by the initial nucleation phase of plating, where the base of the deposit is defined by the surface topography of pitted regions. This suggests that tuning the pit morphology is a potential pathway to improve performance, which could be achieved by electrochemical pretreatments of an electrode surface.⁶⁸

Recently, operando 3-D microscopy has revealed that pits display anisotropic expansion, which is influenced by the electrode microstructure and crystallographic orientation. For example, pit faceting has been observed (Figure 8C).³³ These observations suggest that pit morphology can be tuned through metallurgical processing to further improve performance.

Analogous to the stripping behavior of Li metal in liquid electrolytes, the heterogeneity of the Li/electrolyte interface also plays a critical role in SSBs. However, an important difference is observed in solid-state systems: while the liquid electrolyte can flow to accommodate large volume changes such as Dead Li formation and surface pitting, the nature of the Li/SSE interface is more rigid. As a consequence, changes in surface morphology during stripping can result in significant contact losses, which is a major challenge facing the SSB community.^{78,81,176–180}

Unlike pits, where the liquid electrolyte allows for continual stripping from the pit interior, when voids form at a Li/SSE interface, the loss of contact causes a reduction in interfacial area (Figure 8d).⁹¹ Current theories describe void formation as a competition between the flux of Li^+ ions into the SE and the flux of Li vacancies away from the interface.⁷³ As the current density increases, this flux imbalance can drive vacancy accumulation, resulting in void nucleation. Interestingly, these voids appear to be more stable than one would expect, as they have been observed to remain even when a larger stack pressure than the yield/flow stress of Li is applied.⁷⁸ Furthermore, a recent study has shown that interfacial voids can be “recovered” at elevated temperatures.^{73,179} A detailed understanding of the complex interplay between vacancy diffusion, dislocation motion, and surface diffusion that drives void formation is still lacking, which remains an area of need for fundamental research.

8. FUTURE DIRECTIONS/REMAINING QUESTIONS

The scientific community has made significant progress in recent years toward building a mechanistic understanding of the dynamic evolution of Li metal anodes during cycling. However, there remains a need for additional exploration of these concepts to deepen our understanding and realize the aggressive goal of achieving reversible, safe, and stable Li-metal batteries that can be reproducibly manufactured at scale. Toward this goal, we propose a series of fundamental questions to guide future research:

1. How can we rationally tune the structure/chemistry of the SEI (including artificial SEIs) to control the local current density distribution, thermodynamic stability, and surface diffusion during nucleation?
2. Can we control the reactivity of plated Li with the electrolyte and underlying substrate, throughout the various active cycling and open-circuit rest stages? Is a purely nonreactive boundary condition ideal (or even feasible), and if not, what type of reactions are desirable?
3. What are the spatiotemporal variations in the mechanical stress in Li metal anodes during cycling, including effects from strain rate, temperature, friction, and molar volume?
4. How do the microstructure, crystallographic texture, and defects of Li metal affect the spatial variations in reaction kinetics, growth morphology (anisotropic evolution), and Dead Li formation?
5. Which factors determine the observed variations in dendrite/filament growth morphology?
6. How, when, and where does “Dead Li” form? What are the factors that determine spatial inhomogeneity and current focusing during stripping of nonplanar Li deposits, and how does this eventually lead to the physical, chemical, and/or electronic isolation of Li?

7. What are the detailed mechanisms behind Dead Li recovery, and how does reattachment of isolated Li occur, especially in the presence of an SEI layer, adjacent Dead Li, and liquid/solid electrolyte phases?
8. As we approach high CEs (>99.5%) what are the roles of electrolyte decomposition, corrosion, and Dead Li on the remaining fractional Coulombic inefficiency?
9. How is electrodissolution (stripping) fundamentally different than plating? What determines the observed differences in stripping vs plating behavior throughout cycling (pit/void nucleation and growth, SEI dissolution and collapse, microstructure effects etc.) in both liquid and solid electrolytes.
10. How does the depth-of-discharge (and duty cycle) influence the growth, corrosion, and stripping phenomena described throughout this perspective? Most studies either perform full charge/discharge cycles, or cycle a fixed charge capacity during each half-cycle. However, real-world batteries do not operate under these idealized conditions.

■ AUTHOR INFORMATION

Corresponding Author

Neil P. Dasgupta – Department of Mechanical Engineering and Department of Materials Science & Engineering, University of Michigan, Ann Arbor, Michigan 48109, United States;  orcid.org/0000-0002-5180-4063; Email: ndasgupt@umich.edu

Author

Adrian J. Sanchez – Department of Mechanical Engineering, University of Michigan, Ann Arbor, Michigan 48109, United States

Complete contact information is available at:
<https://pubs.acs.org/10.1021/jacs.3c05715>

Notes

The authors declare no competing financial interest.

■ ACKNOWLEDGMENTS

N.P.D. acknowledges support from the Mechanochemical Understanding of Solid Ion Conductors, an Energy Frontier Research Center funded by the U.S. Department of Energy, Office of Science, Office of Basic Energy Science under grant no. DE-SC0023438.

■ REFERENCES

- (1) Zubi, G.; Dufo-López, R.; Carvalho, M.; Pasaoglu, G. The Lithium-Ion Battery: State of the Art and Future Perspectives. *Renew. Sustain. Energy Rev.* **2018**, *89*, 292–308.
- (2) Cano, Z. P.; Banham, D.; Ye, S.; Hintennach, A.; Lu, J.; Fowler, M.; Chen, Z. Batteries and Fuel Cells for Emerging Electric Vehicle Markets. *Nat. Energy* **2018**, *3* (4), 279–289.
- (3) Saxena, S.; MacDonald, J.; Moura, S. Charging Ahead on the Transition to Electric Vehicles with Standard 120 v Wall Outlets. *Appl. Energy* **2015**, *157* (2015), 720–728.
- (4) Nykvist, B.; Nilsson, M. Rapidly Falling Costs of Battery Packs for Electric Vehicles. *Nat. Clim. Chang.* **2015**, *5* (4), 329–332.
- (5) Gallagher, K. G.; Goebel, S.; Greszler, T.; Mathias, M.; Oelerich, W.; Eroglu, D.; Srinivasan, V. Quantifying the Promise of Lithium-Air Batteries for Electric Vehicles. *Energy Environ. Sci.* **2014**, *7* (5), 1555–1563.
- (6) Lin, D.; Liu, Y.; Cui, Y. Reviving the Lithium Metal Anode for High-Energy Batteries. *Nat. Nanotechnol.* **2017**, *12* (3), 194–206.

- (7) Hobold, G. M.; Lopez, J.; Guo, R.; Minafra, N.; Banerjee, A.; Shirley Meng, Y.; Shao-Horn, Y.; Gallant, B. M. Moving beyond 99.9% Coulombic Efficiency for Lithium Anodes in Liquid Electrolytes. *Nat. Energy* **2021**, *6* (10), 951–960.
- (8) Yang, Y.; Yin, Y.; Davies, D. M.; Zhang, M.; Mayer, M.; Zhang, Y.; Sablina, E. S.; Wang, S.; Lee, J. Z.; Borodin, O.; Rustomji, C. S.; Meng, Y. S. Liquefied Gas Electrolytes for Wide-Temperature Lithium Metal Batteries. *Energy Environ. Sci.* **2020**, *13* (7), 2209–2219.
- (9) Yang, Y.; Davies, D. M.; Yin, Y.; Borodin, O.; Lee, J. Z.; Fang, C.; Olguin, M.; Zhang, Y.; Sablina, E. S.; Wang, X.; Rustomji, C. S.; Meng, Y. S. High-Efficiency Lithium-Metal Anode Enabled by Liquefied Gas Electrolytes. *Joule* **2019**, *3* (8), 1986–2000.
- (10) Wang, H.; Huang, W.; Yu, Z.; Huang, W.; Xu, R.; Zhang, Z.; Bao, Z.; Cui, Y. Efficient Lithium Metal Cycling over a Wide Range of Pressures from an Anion-Derived Solid-Electrolyte Interphase Framework. *ACS Energy Lett.* **2021**, *6* (2), 816–825.
- (11) Kim, M. S.; Zhang, Z.; Rudnicki, P. E.; Yu, Z.; Wang, J.; Wang, H.; Oyakhire, S. T.; Chen, Y.; Kim, S. C.; Zhang, W.; Boyle, D. T.; Kong, X.; Xu, R.; Huang, Z.; Huang, W.; Bent, S. F.; Wang, L. W.; Qin, J.; Bao, Z.; Cui, Y. Suspension Electrolyte with Modified Li⁺ Solvation Environment for Lithium Metal Batteries. *Nat. Mater.* **2022**, *21* (4), 445–454.
- (12) Wang, Z.; Hou, L. P.; Li, Z.; Liang, J. L.; Zhou, M. Y.; Zhao, C. Z.; Zeng, X.; Li, B. Q.; Chen, A.; Zhang, X. Q.; Dong, P.; Zhang, Y.; Huang, J. Q.; Zhang, Q. Highly Soluble Organic Nitrate Additives for Practical Lithium Metal Batteries. *Carbon Energy* **2023**, *5* (1), 1–9.
- (13) Adams, B. D.; Carino, E. V.; Connell, J. G.; Han, K. S.; Cao, R.; Chen, J.; Zheng, J.; Li, Q.; Mueller, K. T.; Henderson, W. A.; Zhang, J. G. Long Term Stability of Li-S Batteries Using High Concentration Lithium Nitrate Electrolytes. *Nano Energy* **2017**, *40*, 607–617.
- (14) Qian, J.; Henderson, W. A.; Xu, W.; Bhattacharya, P.; Engelhard, M.; Borodin, O.; Zhang, J.-G. High Rate and Stable Cycling of Lithium Metal Anode. *Nat. Commun.* **2015**, *6* (1), No. 6362.
- (15) Qian, J.; Xu, W.; Bhattacharya, P.; Engelhard, M.; Henderson, W. A.; Zhang, Y.; Zhang, J. G. Dendrite-Free Li Deposition Using Trace-Amounts of Water as an Electrolyte Additive. *Nano Energy* **2015**, *15*, 135–144.
- (16) Yu, Z.; Rudnicki, P. E.; Zhang, Z.; Huang, Z.; Celik, H.; Oyakhire, S. T.; Chen, Y.; Kong, X.; Kim, S. C.; Xiao, X.; Wang, H.; Zheng, Y.; Kamat, G. A.; Kim, M. S.; Bent, S. F.; Qin, J.; Cui, Y.; Bao, Z. Rational Solvent Molecule Tuning for High-Performance Lithium Metal Battery Electrolytes. *Nat. Energy* **2022**, *7* (1), 94–106.
- (17) Jeoun, Y.; Kim, K.; Kim, S.-Y.; Lee, S.-H.; Huh, S.-H.; Kim, S. H.; Huang, X.; Sung, Y.-E.; Abruna, H. D.; Yu, S.-H. Surface Roughness-Independent Homogeneous Lithium Plating in Synergetic Conditioned Electrolyte. *ACS Energy Lett.* **2022**, *7* (7), 2219–2227.
- (18) Xie, J.; Sun, S. Y.; Chen, X.; Hou, L. P.; Li, B. Q.; Peng, H. J.; Huang, J. Q.; Zhang, X. Q.; Zhang, Q. Fluorinating the Solid Electrolyte Interphase by Rational Molecular Design for Practical Lithium-Metal Batteries. *Angew. Chemie - Int. Ed.* **2022**, *61* (29), No. e202204776, DOI: 10.1002/anie.202204776.
- (19) Liu, H.; Cheng, X.; Zhang, R.; Shi, P.; Shen, X.; Chen, X.; Li, T.; Huang, J.; Zhang, Q. Mesoporous Graphene Hosts for Dendrite-Free Lithium Metal Anode in Working Rechargeable Batteries. *Trans. Tianjin Univ.* **2020**, *26* (2), 127–134.
- (20) Chi, S.-S.; Liu, Y.; Song, W. L.; Fan, L. Z.; Zhang, Q. Prestoring Lithium into Stable 3D Nickel Foam Host as Dendrite-Free Lithium Metal Anode. *Adv. Funct. Mater.* **2017**, *27* (24), 1–10.
- (21) Chen, H.; Pei, A.; Wan, J.; Lin, D.; Vilá, R.; Wang, H.; Mackanic, D.; Steinrück, H. G.; Huang, W.; Li, Y.; Yang, A.; Xie, J.; Wu, Y.; Wang, H.; Cui, Y. Tortuosity Effects in Lithium-Metal Host Anodes. *Joule* **2020**, *4* (4), 938–952.
- (22) Chen, H.; Yang, Y.; Boyle, D. T.; Jeong, Y. K.; Xu, R.; de Vasconcelos, L. S.; Huang, Z.; Wang, H.; Wang, H.; Huang, W.; Li, H.; Wang, J.; Gu, H.; Matsumoto, R.; Motohashi, K.; Nakayama, Y.; Zhao, K.; Cui, Y. Free-Standing Ultrathin Lithium Metal–Graphene Oxide Host Foils with Controllable Thickness for Lithium Batteries. *Nat. Energy* **2021**, *6* (8), 790–798.
- (23) Zheng, G.; Lee, S. W.; Liang, Z.; Lee, H. W.; Yan, K.; Yao, H.; Wang, H.; Li, W.; Chu, S.; Cui, Y. Interconnected Hollow Carbon Nanospheres for Stable Lithium Metal Anodes. *Nat. Nanotechnol.* **2014**, *9* (8), 618–623.
- (24) Lu, L.-L.; Ge, J.; Yang, J.-N.; Chen, S.-M.; Yao, H.-B.; Zhou, F.; Yu, S.-H. Free-Standing Copper Nanowire Network Current Collector for Improving Lithium Anode Performance. *Nano Lett.* **2016**, *16* (7), 4431–4437.
- (25) Zhang, Z.; Xu, X.; Wang, S.; Peng, Z.; Liu, M.; Zhou, J.; Shen, C.; Wang, D. Li₂O-Reinforced Cu Nanoclusters as Porous Structure for Dendrite-Free and Long-Lifespan Lithium Metal Anode. *ACS Appl. Mater. Interfaces* **2016**, *8* (40), 26801–26808.
- (26) Harlow, J. E.; Ma, X.; Li, J.; Logan, E.; Liu, Y.; Zhang, N.; Ma, L.; Glazier, S. L.; Cormier, M. M. E.; Genovese, M.; Buteau, S.; Cameron, A.; Stark, J. E.; Dahn, J. R. A Wide Range of Testing Results on an Excellent Lithium-Ion Cell Chemistry to Be Used as Benchmarks for New Battery Technologies. *J. Electrochem. Soc.* **2019**, *166* (13), A3031–A3044.
- (27) Lang, S.; Yu, S. H.; Feng, X.; Krumov, M. R.; Abruna, H. D. Understanding the Lithium–Sulfur Battery Redox Reactions via Operando Confocal Raman Microscopy. *Nat. Commun.* **2022**, *13* (1), 1–11.
- (28) Sanchez, A. J.; Kazyak, E.; Chen, Y.; Chen, K. H.; Pattison, E. R.; Dasgupta, N. P. Plan-View Operando Video Microscopy of Li Metal Anodes: Identifying the Coupled Relationships among Nucleation, Morphology, and Reversibility. *ACS Energy Lett.* **2020**, *5* (3), 994–1004.
- (29) KüPfers, V.; Kolek, M.; Bieker, P.; Winter, M.; Brunklaus, G. In Situ ⁷Li-NMR Analysis of Lithium Metal Surface Deposits with Varying Electrolyte Compositions and Concentrations. *Phys. Chem. Chem. Phys.* **2019**, *21* (47), 26084–26094.
- (30) Krueger, B.; Balboa, L.; Dohmann, J. F.; Winter, M.; Bieker, P.; Wittstock, G. Solid Electrolyte Interphase Evolution on Lithium Metal Electrodes Followed by Scanning Electrochemical Microscopy Under Realistic Battery Cycling Current Densities. *ChemElectroChem.* **2020**, *7* (17), 3590–3596.
- (31) Xiang, Y.; Tao, M.; Zhong, G.; Liang, Z.; Zheng, G.; Huang, X.; Liu, X.; Jin, Y.; Xu, N.; Armand, M.; Zhang, J. G.; Xu, K.; Fu, R.; Yang, Y. Quantitatively Analyzing the Failure Processes of Rechargeable Li Metal Batteries. *Sci. Adv.* **2021**, *7* (46), 1–12.
- (32) Shen, F.; Dixit, M. B.; Xiao, X.; Hatzell, K. B. Effect of Pore Connectivity on Li Dendrite Propagation within LLZO Electrolytes Observed with Synchrotron X-Ray Tomography. *ACS Energy Lett.* **2018**, *3* (4), 1056–1061.
- (33) Sanchez, A. J.; Kazyak, E.; Chen, Y.; Lasso, J.; Dasgupta, N. P. Lithium Stripping: Anisotropic Evolution and Faceting of Pits Revealed by Operando 3-D Microscopy. *J. Mater. Chem. A* **2021**, *9* (37), 21013–21023.
- (34) Hong, Y.-S.; Li, N.; Chen, H.; Wang, P.; Song, W.-L.; Fang, D. In Operando Observation of Chemical and Mechanical Stability of Li and Na Dendrites under Quasi-Zero Electrochemical Field. *Energy Storage Mater.* **2018**, *11*, 118–126.
- (35) Menkin, S.; O’Keefe, C. A.; Gunnarsdóttir, A. B.; Dey, S.; Pesci, F. M.; Shen, Z.; Aguadero, A.; Grey, C. P. Toward an Understanding of SEI Formation and Lithium Plating on Copper in Anode-Free Batteries. *J. Phys. Chem. C* **2021**, *125* (30), 16719–16732.
- (36) Gunnarsdóttir, A. B.; Vema, S.; Menkin, S.; Marbella, L. E.; Grey, C. P. Investigating the Effect of a Fluoroethylene Carbonate Additive on Lithium Deposition and the Solid Electrolyte Interphase in Lithium Metal Batteries Using: In Situ NMR Spectroscopy. *J. Mater. Chem. A* **2020**, *8* (30), 14975–14992.
- (37) Geise, N. R.; Kasse, R. M.; Nelson Weker, J.; Steinrück, H. G.; Toney, M. F. Quantification of Efficiency in Lithium Metal Negative Electrodes via Operando X-Ray Diffraction. *Chem. Mater.* **2021**, *33* (18), 7537–7545.
- (38) Kushima, A.; So, K. P.; Su, C.; Bai, P.; Kuriyama, N.; Maebashi, T.; Fujiwara, Y.; Bazant, M. Z.; Li, J. Liquid Cell Transmission

- Electron Microscopy Observation of Lithium Metal Growth and Dissolution: Root Growth, Dead Lithium and Lithium Flotsams. *Nano Energy* 2017, 32, 271–279.
- (39) Bai, P.; Li, J.; Brushett, F. R.; Bazant, M. Z. Transition of Lithium Growth Mechanisms in Liquid Electrolytes. *Energy Environ. Sci.* 2016, 9 (10), 3221–3229.
- (40) Kazyak, E.; Garcia-Mendez, R.; LePage, W. S.; Sharifi, A.; Davis, A. L.; Sanchez, A. J.; Chen, K. H.; Haslam, C.; Sakamoto, J.; Dasgupta, N. P. Li Penetration in Ceramic Solid Electrolytes: Operando Microscopy Analysis of Morphology, Propagation, and Reversibility. *Matter* 2020, 2 (4), 1025–1048.
- (41) Wood, K. N.; Noked, M.; Dasgupta, N. P. Lithium Metal Anodes: Toward an Improved Understanding of Coupled Morphological, Electrochemical, and Mechanical Behavior. *ACS Energy Lett.* 2017, 2 (3), 664–672.
- (42) Fang, C.; Wang, X.; Meng, Y. S. Key Issues Hindering a Practical Lithium-Metal Anode. *Trends Chem.* 2019, 1 (2), 152–158.
- (43) Huang, W. Z.; Zhao, C. Z.; Wu, P.; Yuan, H.; Feng, W. E.; Liu, Z. Y.; Lu, Y.; Sun, S.; Fu, Z. H.; Hu, J. K.; Yang, S. J.; Huang, J. Q.; Zhang, Q. Anode-Free Solid-State Lithium Batteries: A Review. *Adv. Energy Mater.* 2022, 12 (26), 1–16.
- (44) Paul, P. P.; McShane, E. J.; Colclasure, A. M.; Balsara, N.; Brown, D. E.; Cao, C.; Chen, B. R.; Chinnam, P. R.; Cui, Y.; Dufek, E. J.; Finegan, D. P.; Gillard, S.; Huang, W.; Konz, Z. M.; Kostecki, R.; Liu, F.; Lubner, S.; Prasher, R.; Preefer, M. B.; Qian, J.; Rodrigues, M. T. F.; Schnabel, M.; Son, S. B.; Srinivasan, V.; Steinrück, H. G.; Tanim, T. R.; Toney, M. F.; Tong, W.; Usseglio-Viretta, F.; Wan, J.; Yusuf, M.; McCloskey, B. D.; Nelson Weker, J. A Review of Existing and Emerging Methods for Lithium Detection and Characterization in Li-Ion and Li-Metal Batteries. *Adv. Energy Mater.* 2021, 11 (17), 1–29.
- (45) Liang, H.; Wang, L.; Sheng, L.; Xu, H.; Song, Y.; He, X. Focus on the Electroplating Chemistry of Li Ions in Nonaqueous Liquid Electrolytes: Toward Stable Lithium Metal Batteries. *Electrochem. Energy Rev.* 2022, 5, 23 DOI: 10.1007/s41918-022-00158-2.
- (46) Liaw, B.; Pawar, G.; Meng, Y. S.; Fang, C.; Lu, B. Perspective—Lithium Metal Nucleation and Growth on Conductive Substrates: A Multi-Scale Understanding from Atomistic, Nano-, Meso-, to Micro-Scales. *J. Electrochem. Soc.* 2022, 169 (11), No. 112505.
- (47) Liu, J.; Bao, Z.; Cui, Y.; Dufek, E. J.; Goodenough, J. B.; Khalifah, P.; Li, Q.; Liaw, B. Y.; Liu, P.; Manthiram, A.; Meng, Y. S.; Subramanian, V. R.; Toney, M. F.; Viswanathan, V. V.; Whittingham, M. S.; Xiao, J.; Xu, W.; Yang, J.; Yang, X. Q.; Zhang, J. G. Pathways for Practical High-Energy Long-Cycling Lithium Metal Batteries. *Nat. Energy* 2019, 4 (3), 180–186.
- (48) Wang, H.; Yu, Z.; Kong, X.; Kim, S. C.; Boyle, D. T.; Qin, J.; Bao, Z.; Cui, Y. Liquid Electrolyte: The Nexus of Practical Lithium Metal Batteries. *Joule* 2022, 6 (3), 588–616.
- (49) Zheng, J.; Kim, M. S.; Tu, Z.; Choudhury, S.; Tang, T.; Archer, L. A. Regulating Electrodeposition Morphology of Lithium: Towards Commercially Relevant Secondary Li Metal Batteries. *Chem. Soc. Rev.* 2020, 49 (9), 2701–2750.
- (50) Liu, Y.; Elias, Y.; Meng, J.; Aurbach, D.; Zou, R.; Xia, D.; Pang, Q. Electrolyte Solutions Design for Lithium-Sulfur Batteries. *Joule* 2021, 5 (9), 2323–2364.
- (51) Lewis, J. A.; Cavallaro, K. A.; Liu, Y.; McDowell, M. T. The Promise of Alloy Anodes for Solid-State Batteries. *Joule* 2022, 6 (7), 1418–1430.
- (52) Zhang, J. G.; Xu, W.; Xiao, J.; Cao, X.; Liu, J. Lithium Metal Anodes with Nonaqueous Electrolytes. *Chem. Rev.* 2020, 120 (24), 13312–13348.
- (53) Bi, C.-X.; Hou, L.-P.; Li, Z.; Zhao, M.; Zhang, X.-Q.; Li, B.-Q.; Zhang, Q.; Huang, J.-Q. Protecting Lithium Metal Anodes in Lithium–Sulfur Batteries: A Review. *Energy Mater. Adv.* 2023, 4, 1–23.
- (54) Pei, A.; Zheng, G.; Shi, F.; Li, Y.; Cui, Y. Nanoscale Nucleation and Growth of Electrodeposited Lithium Metal. *Nano Lett.* 2017, 17 (2), 1132–1139.
- (55) Biswal, P.; Stalin, S.; Kludze, A.; Choudhury, S.; Archer, L. A. Nucleation and Early Stage Growth of Li Electrodeposits. *Nano Lett.* 2019, 19 (11), 8191–8200.
- (56) Wood, K. N.; Kazyak, E.; Chadwick, A. F.; Chen, K. H.; Zhang, J. G.; Thornton, K.; Dasgupta, N. P. Dendrites and Pits: Untangling the Complex Behavior of Lithium Metal Anodes through Operando Video Microscopy. *ACS Cent. Sci.* 2016, 2 (11), 790–801.
- (57) Zhang, Z.; Li, Y.; Xu, R.; Zhou, W.; Li, Y.; Oyakhire, S. T.; Wu, Y.; Xu, J.; Wang, H.; Yu, Z.; Boyle, D. T.; Huang, W.; Ye, Y.; Chen, H.; Wan, J.; Bao, Z.; Chiu, W.; Cui, Y. Capturing the Swelling of Solid-Electrolyte Interphase in Lithium Metal Batteries. *Science* (80-.). 2022, 375 (6576), 66–70.
- (58) Aurbach, D. Review of Selected Electrode–Solution Interactions Which Determine the Performance of Li and Li Ion Batteries. *J. Power Sources* 2000, 89 (2), 206–218.
- (59) Yoon, I.; Jurng, S.; Abraham, D. P.; Lucht, B. L.; Guduru, P. R. Measurement of Mechanical and Fracture Properties of Solid Electrolyte Interphase on Lithium Metal Anodes in Lithium Ion Batteries. *Energy Storage Mater.* 2020, 25, 296–304.
- (60) Gunnarsdóttir, A. B.; Amanchukwu, C. V.; Menkin, S.; Grey, C. P. Noninvasive in Situ NMR Study of “Dead Lithium” Formation and Lithium Corrosion in Full-Cell Lithium Metal Batteries. *J. Am. Chem. Soc.* 2020, 142 (49), 20814–20827.
- (61) Liu, F.; Xu, R.; Wu, Y.; Boyle, D. T.; Yang, A.; Xu, J.; Zhu, Y.; Ye, Y.; Yu, Z.; Zhang, Z.; Xiao, X.; Huang, W.; Wang, H.; Chen, H.; Cui, Y. Dynamic Spatial Progression of Isolated Lithium during Battery Operations. *Nature* 2021, 600 (7890), 659–663.
- (62) Tewari, D.; Rangarajan, S. P.; Balbuena, P. B.; Barsukov, Y.; Mukherjee, P. P. Mesoscale Anatomy of Dead Lithium Formation. *J. Phys. Chem. C* 2020, 124 (12), 6502–6511.
- (63) Chen, K.-H.; Wood, K. N.; Kazyak, E.; LePage, W. S.; Davis, A. L.; Sanchez, A. J.; Dasgupta, N. P. Dead Lithium: Mass Transport Effects on Voltage, Capacity, and Failure of Lithium Metal Anodes. *J. Mater. Chem. A* 2017, 5 (23), 11671–11681.
- (64) Fang, C.; Li, J.; Zhang, M.; Zhang, Y.; Yang, F.; Lee, J. Z.; Lee, M.-H.; Alvarado, J.; Schroeder, M. A.; Yang, Y.; Lu, B.; Williams, N.; Ceja, M.; Yang, L.; Cai, M.; Gu, J.; Xu, K.; Wang, X.; Meng, Y. S. Quantifying Inactive Lithium in Lithium Metal Batteries. *Nature* 2019, 572 (7770), 511–515.
- (65) Shi, F.; Pei, A.; Boyle, D. T.; Xie, J.; Yu, X.; Zhang, X.; Cui, Y. Lithium Metal Stripping beneath the Solid Electrolyte Interphase. *Proc. Natl. Acad. Sci. U. S. A.* 2018, 115 (34), 8529–8534.
- (66) Huang, Y.; Pan, R.; Rehnlund, D.; Wang, Z.; Nyholm, L. First-Cycle Oxidative Generation of Lithium Nucleation Sites Stabilizes Lithium-Metal Electrodes. *Adv. Energy Mater.* 2021, 11 (9), No. 2003674.
- (67) Gireaud, L.; Grugeon, S.; Laruelle, S.; Yrieix, B.; Tarascon, J.-M. Lithium Metal Stripping/Plating Mechanisms Studies: A Metallurgical Approach. *Electrochim. commun.* 2006, 8 (10), 1639–1649.
- (68) Aleshin, A.; Bravo, S.; Redquest, K.; Wood, K. N. Rapid Oxidation and Reduction of Lithium for Improved Cycling Performance and Increased Homogeneity. *ACS Appl. Mater. Interfaces* 2021, 13 (2), 2654–2661.
- (69) LePage, W. S.; Chen, Y.; Kazyak, E.; Chen, K.-H.; Sanchez, A. J.; Poli, A.; Arruda, E. M.; Thouless, M. D.; Dasgupta, N. P. Lithium Mechanics: Roles of Strain Rate and Temperature and Implications for Lithium Metal Batteries. *J. Electrochem. Soc.* 2019, 166 (2), A89–A97.
- (70) Xu, C.; Ahmad, Z.; Aryanfar, A.; Viswanathan, V.; Greer, J. R. Enhanced Strength and Temperature Dependence of Mechanical Properties of Li at Small Scales and Its Implications for Li Metal Anodes. *Proc. Natl. Acad. Sci. U. S. A.* 2017, 114 (1), 57–61.
- (71) Herbert, E. G.; Hackney, S. A.; Thole, V.; Dudney, N. J.; Phani, P. S. Nanoindentation of High-Purity Vapor Deposited Lithium Films: A Mechanistic Rationalization of Diffusion-Mediated Flow. *J. Mater. Res.* 2018, 33 (10), 1347–1360.
- (72) Fang, C.; Lu, B.; Pawar, G.; Zhang, M.; Cheng, D.; Chen, S.; Ceja, M.; Doux, J.-M.; Musrock, H.; Cai, M.; Liaw, B.; Meng, Y. S.

- Pressure-Tailored Lithium Deposition and Dissolution in Lithium Metal Batteries **2021**, *6* (10), 987–994.
- (73) Krauskopf, T.; Hartmann, H.; Zeier, W. G.; Janek, J. Toward a Fundamental Understanding of the Lithium Metal Anode in Solid-State Batteries - An Electrochemo-Mechanical Study on the Garnet-Type Solid Electrolyte Li_{6.25}Al_{0.25}La₃Zr₂O₁₂. *ACS Appl. Mater. Interfaces* **2019**, *11* (15), 14463–14477.
- (74) Haslam, C. G.; Wolfenstine, J. B.; Sakamoto, J. The Effect of Aspect Ratio on the Mechanical Behavior of Li Metal in Solid-State Cells. *J. Power Sources* **2022**, *520*, No. 230831.
- (75) Masias, A.; Felten, N.; Garcia-Mendez, R.; Wolfenstine, J.; Sakamoto, J. Elastic, Plastic, and Creep Mechanical Properties of Lithium Metal. *J. Mater. Sci.* **2019**, *54* (3), 2585–2600.
- (76) Fincher, C. D.; Ojeda, D.; Zhang, Y.; Pharr, G. M.; Pharr, M. Mechanical Properties of Metallic Lithium: From Nano to Bulk Scales. *Acta Mater.* **2020**, *186*, 215–222.
- (77) Porz, L.; Swamy, T.; Sheldon, B. W.; Rettenwander, D.; Frömling, T.; Thaman, H. L.; Berends, S.; Uecker, R.; Carter, W. C.; Chiang, Y. M. Mechanism of Lithium Metal Penetration through Inorganic Solid Electrolytes. *Adv. Energy Mater.* **2017**, *7* (20), 1–12.
- (78) Wang, M. J.; Choudhury, R.; Sakamoto, J. Characterizing the Li-Solid-Electrolyte Interface Dynamics as a Function of Stack Pressure and Current Density. *Joule* **2019**, *3* (9), 2165–2178.
- (79) Doux, J. M.; Nguyen, H.; Tan, D. H. S.; Banerjee, A.; Wang, X.; Wu, E. A.; Jo, C.; Yang, H.; Meng, Y. S. Stack Pressure Considerations for Room-Temperature All-Solid-State Lithium Metal Batteries. *Adv. Energy Mater.* **2020**, *10* (1), 1–6.
- (80) Krauskopf, T.; Mogwitz, B.; Rosenbach, C.; Zeier, W. G.; Janek, J. Diffusion Limitation of Lithium Metal and Li–Mg Alloy Anodes on LLZO Type Solid Electrolytes as a Function of Temperature and Pressure. *Adv. Energy Mater.* **2019**, *9* (44), 1902568 DOI: [10.1002/aenm.201902568](https://doi.org/10.1002/aenm.201902568).
- (81) Zhang, X.; Wang, Q. J.; Harrison, K. L.; Roberts, S. A.; Harris, S. J. Pressure-Driven Interface Evolution in Solid-State Lithium Metal Batteries. *Cell Reports Phys. Sci.* **2020**, *1* (2), No. 100012.
- (82) Peled, E.; Menkin, S. Review—SEI: Past, Present and Future. *J. Electrochem. Soc.* **2017**, *164* (7), A1703–A1719.
- (83) Wang, X.; Pawar, G.; Li, Y.; Ren, X.; Zhang, M.; Lu, B.; Banerjee, A.; Liu, P.; Dufek, E. J.; Zhang, J.-G.; Xiao, J.; Liu, J.; Meng, Y. S.; Liaw, B. Glassy Li Metal Anode for High-Performance Rechargeable Li Batteries. *Nat. Mater.* **2020**, *19* (12), 1339–1345.
- (84) Otto, S.-K.; Moryson, Y.; Krauskopf, T.; Peppler, K.; Sann, J.; Janek, J.; Henss, A. In-Depth Characterization of Lithium-Metal Surfaces with XPS and ToF-SIMS: Toward Better Understanding of the Passivation Layer. *Chem. Mater.* **2021**, *33* (3), 859–867.
- (85) Wang, X.; Zhang, M.; Alvarado, J.; Wang, S.; Sina, M.; Lu, B.; Bouwer, J.; Xu, W.; Xiao, J.; Zhang, J. G.; Liu, J.; Meng, Y. S. New Insights on the Structure of Electrochemically Deposited Lithium Metal and Its Solid Electrolyte Interphases via Cryogenic TEM. *Nano Lett.* **2017**, *17* (12), 7606–7612.
- (86) Huang, W.; Boyle, D. T.; Li, Y.; Li, Y.; Pei, A.; Chen, H.; Cui, Y. Nanostructural and Electrochemical Evolution of the Solid-Electrolyte Interphase on CuO Nanowires Revealed by Cryogenic-Electron Microscopy and Impedance Spectroscopy. *ACS Nano* **2019**, *13* (1), 737–744.
- (87) Oyakhire, S. T.; Zhang, W.; Yu, Z.; Holmes, S. E.; Sayavong, P.; Kim, S. C.; Boyle, D. T.; Kim, M. S.; Zhang, Z.; Cui, Y.; Bent, S. F. Correlating the Formation Protocols of Solid Electrolyte Interphases with Practical Performance Metrics in Lithium Metal Batteries. *ACS Energy Lett.* **2023**, *8* (1), 869–877.
- (88) Yuan, S.; Weng, S.; Wang, F.; Dong, X.; Wang, Y.; Wang, Z.; Shen, C.; Bao, J. L.; Wang, X.; Xia, Y. Revisiting the Designing Criteria of Advanced Solid Electrolyte Interphase on Lithium Metal Anode under Practical Condition. *Nano Energy* **2021**, *83*, 105847.
- (89) Boyle, D. T.; Kong, X.; Pei, A.; Rudnicki, P. E.; Shi, F.; Huang, W.; Bao, Z.; Qin, J.; Cui, Y. Transient Voltammetry with Ultramicroelectrodes Reveals the Electron Transfer Kinetics of Lithium Metal Anodes. *ACS Energy Lett.* **2020**, *5* (3), 701–709.
- (90) Tao, R.; Bi, X.; Li, S.; Yao, Y.; Wu, F.; Wang, Q.; Zhang, C.; Lu, J. Kinetics Tuning the Electrochemistry of Lithium Dendrites Formation in Lithium Batteries through Electrolytes. *ACS Appl. Mater. Interfaces* **2017**, *9* (8), 7003–7008.
- (91) Krauskopf, T.; Mogwitz, B.; Hartmann, H.; Singh, D. K.; Zeier, W. G.; Janek, J. The Fast Charge Transfer Kinetics of the Lithium Metal Anode on the Garnet-Type Solid Electrolyte Li_{6.25}Al_{0.25}La₃Zr₂O₁₂. *Adv. Energy Mater.* **2020**, *10* (27), 2000945 DOI: [10.1002/aenm.202000945](https://doi.org/10.1002/aenm.202000945).
- (92) Zhang, S.; Yang, G.; Liu, S.; Li, X.; Wang, X.; Wang, Z.; Chen, L. Understanding the Dropping of Lithium Plating Potential in Carbonate Electrolyte. *Nano Energy* **2020**, *70*, No. 104486.
- (93) Jin, C.-B.; Yao, N.; Xiao, Y.; Xie, J.; Li, Z.; Chen, X.; Li, B.-Q.; Zhang, X.-Q.; Huang, J.-Q.; Zhang, Q. Taming Solvent–Solute Interaction Accelerates Interfacial Kinetics in Low-Temperature Lithium–Metal Batteries. *Adv. Mater.* **2023**, *35* (3), 1–9.
- (94) Lu, Y.; Zhao, C. Z.; Huang, J. Q.; Zhang, Q. The Timescale Identification Decoupling Complicated Kinetic Processes in Lithium Batteries. *Joule* **2022**, *6* (6), 1172–1198.
- (95) Plieth, W. *Electrochemistry for Materials Science*; Elsevier: Amsterdam, 2008, pp 195–229 DOI: [10.1016/B978-0-444-52792-9.X5001-5](https://doi.org/10.1016/B978-0-444-52792-9.X5001-5).
- (96) Budevski, E.; Staikov, G.; Lorenz, W. J. *Electrochemical Phase Formation and Growth. An Introduction to the Initial Stages of Metal Deposition*; VCH Verlagsgesellschaft: Weinheim, 1996, pp 149–199.
- (97) Ely, D. R.; Garcia, R. E. Heterogeneous Nucleation and Growth of Lithium Electrodeposits on Negative Electrodes. *J. Electrochem. Soc.* **2013**, *160* (4), A662–A668.
- (98) Mistry, A.; Mukherjee, P. P. Molar Volume Mismatch: A Malefactor for Irregular Metallic Electrodeposition with Solid Electrolytes. *J. Electrochem. Soc.* **2020**, *167* (8), No. 082510.
- (99) Sandoval, S. E.; Cortes, F. J. Q.; Klein, E. J.; Lewis, J. A.; Shetty, P. P.; Yeh, D.; McDowell, M. T. Understanding the Effects of Alloy Films on the Electrochemical Behavior of Lithium Metal Anodes with Operando Optical Microscopy. *J. Electrochem. Soc.* **2021**, *168* (10), No. 100517.
- (100) Yan, K.; Lu, Z.; Lee, H. W.; Xiong, F.; Hsu, P. C.; Li, Y.; Zhao, J.; Chu, S.; Cui, Y. Selective Deposition and Stable Encapsulation of Lithium through Heterogeneous Seeded Growth. *Nat. Energy* **2016**, *1* (3), 16010.
- (101) Gamborg, Y. D.; Zangari, G. *Theory and Practice of Metal Electrodeposition*; Springer: New York, NY, 2011, 97–122 DOI: [10.1007/978-1-4419-9669-5](https://doi.org/10.1007/978-1-4419-9669-5).
- (102) Kolesnikov, A.; Zhou, D.; Kolek, M.; Jimenez, J. P. B.; Bieker, P.; Winter, M.; Stan, M. C. Lithium-Powder Based Electrodes Modified with ZnI₂ for Enhanced Electrochemical Performance of Lithium–Metal Batteries. *J. Electrochem. Soc.* **2019**, *166* (8), A1400–A1407.
- (103) Zhang, N.; Yu, S. H.; Abruña, H. D. Regulating Lithium Nucleation and Growth by Zinc Modified Current Collectors. *Nano Res.* **2020**, *13* (1), 45–51.
- (104) Stan, M. C.; Becking, J.; Kolesnikov, A.; Wankmiller, B.; Frerichs, J. E.; Hansen, M. R.; Bieker, P.; Kolek, M.; Winter, M. Sputter Coating of Lithium Metal Electrodes with Lithiophilic Metals for Homogeneous and Reversible Lithium Electrodeposition and Electrodissolution. *Mater. Today* **2020**, *39*, 137–145.
- (105) Hao, F.; Vishnugopi, B. S.; Wang, H.; Mukherjee, P. P. Chemomechanical Interactions Dictate Lithium Surface Diffusion Kinetics in the Solid Electrolyte Interphase. *Langmuir* **2022**, *38* (18), 5472–5480.
- (106) Xin, X.; Ito, K.; Dutta, A.; Kubo, Y. Dendrite-Free Epitaxial Growth of Lithium Metal during Charging in Li–O₂ Batteries. *Angew. Chemie - Int. Ed.* **2018**, *57* (40), 13206–13210.
- (107) Lin, L.; Suo, L.; Hu, Y.-s.; Li, H.; Huang, X.; Chen, L. Epitaxial Induced Plating Current-Collector Lasting Lifespan of Anode-Free Lithium Metal Battery. *Adv. Energy Mater.* **2021**, *11* (9), 2003709 DOI: [10.1002/aenm.202003709](https://doi.org/10.1002/aenm.202003709).
- (108) Shen, X.; Zhang, J.; Chen, H.; Sun, H.; Zhang, L.; Li, B.; Zhang, H.; Li, X.; Li, S.; Zhu, J.; Duan, X. Microenvironment

Engineering for Guiding Spatially and Epitaxially Uniform Lithium Plating in Lithium Metal Batteries. *Energy Storage Mater.* **2023**, *61*, 102878.

(109) Carmona, E. A.; Wang, M. J.; Song, Y.; Sakamoto, J.; Albertus, P. The Effect of Mechanical State on the Equilibrium Potential of Alkali Metal/Ceramic Single-Ion Conductor Systems. *Adv. Energy Mater.* **2021**, *11* (29), 1–7.

(110) Kazyak, E.; Wang, M. J.; Lee, K.; Yadavalli, S.; Sanchez, A. J.; Thouless, M. D.; Sakamoto, J.; Dasgupta, N. P. Understanding the Electro-Chemo-Mechanics of Li Plating in Anode-Free Solid-State Batteries with Operando 3D Microscopy. *Matter* **2022**, *5* (11), 3912–3934.

(111) Sharifi, A.; Kazyak, E.; Davis, A. L.; Yu, S.; Thompson, T.; Siegel, D. J.; Dasgupta, N. P.; Sakamoto, J. Surface Chemistry Mechanism of Ultra-Low Interfacial Resistance in the Solid-State Electrolyte Li₇La₃Zr₂O₁₂. *Chem. Mater.* **2017**, *29* (18), 7961–7968.

(112) Hope, M. A.; Rinkel, B. L. D.; Gunnarsdóttir, A. B.; Märker, K.; Menkin, S.; Paul, S.; Sergeyev, I. V.; Grey, C. P. Selective NMR Observation of the SEI–Metal Interface by Dynamic Nuclear Polarisation from Lithium Metal. *Nat. Commun.* **2020**, *11* (1), 2224

DOI: 10.1038/s41467-020-16114-x.

(113) Kim, K.; Siegel, D. J. Predicting Wettability and the Electrochemical Window of Lithium-Metal/Solid Electrolyte Interfaces. *ACS Appl. Mater. Interfaces* **2019**, *11* (43), 39940–39950.

(114) Nagy, K. S.; Kazemiabnabi, S.; Thornton, K.; Siegel, D. J. Thermodynamic Overpotentials and Nucleation Rates for Electrodeposition on Metal Anodes. *ACS Appl. Mater. Interfaces* **2019**, *11* (8), 7954–7964.

(115) Meyerson, M. L.; Sheavly, J. K.; Dolocan, A.; Griffin, M. P.; Pandit, A. H.; Rodriguez, R.; Stephens, R. M.; Vanden Bout, D. A.; Heller, A.; Mullins, C. B. The Effect of Local Lithium Surface Chemistry and Topography on Solid Electrolyte Interphase Composition and Dendrite Nucleation. *J. Mater. Chem. A* **2019**, *7* (24), 14882–14894.

(116) Kim, Y. J.; Jin, H. S.; Lee, D. H.; Choi, J.; Jo, W.; Noh, H.; Lee, J.; Chu, H.; Kwack, H.; Ye, F.; Lee, H.; Ryou, M. H.; Kim, H. T. Guided Lithium Deposition by Surface Micro-Patterning of Lithium-Metal Electrodes. *ChemElectroChem.* **2018**, *5* (21), 3169–3175.

(117) Ryou, M.-H.; Lee, Y. M.; Lee, Y.; Winter, M.; Bieker, P. Mechanical Surface Modification of Lithium Metal: Towards Improved Li Metal Anode Performance by Directed Li Plating. *Adv. Funct. Mater.* **2015**, *25* (6), 834–841.

(118) Li, Y.; Li, Y.; Pei, A.; Yan, K.; Sun, Y.; Wu, C. L.; Joubert, L. M.; Chin, R.; Koh, A. L.; Yu, Y.; Perrino, J.; Butz, B.; Chu, S.; Cui, Y. Atomic Structure of Sensitive Battery Materials and Interfaces Revealed by Cryo-Electron Microscopy. *Science* (80-.). **2017**, *358* (6362), 506–510.

(119) Vishnugopi, B. S.; Hao, F.; Verma, A.; Mukherjee, P. P. Double-Edged Effect of Temperature on Lithium Dendrites. *ACS Appl. Mater. Interfaces* **2020**, *12* (21), 23931–23938.

(120) Meyer, J. M.; Harrison, K. L.; Mukherjee, P. P.; Roberts, S. A. Developing a Model for the Impact of Non-Conformal Lithium Contact on Electro-Chemo-Mechanics and Dendrite Growth. *Cell Reports Phys. Sci.* **2023**, *4* (4), No. 101364.

(121) Bai, P.; Guo, J.; Wang, M.; Kushima, A.; Su, L.; Li, J.; Brushett, F. R.; Bazant, M. Z. Interactions between Lithium Growths and Nanoporous Ceramic Separators. *Joule* **2018**, *2* (11), 2434–2449.

(122) Oyakhire, S. T.; Zhang, W.; Shin, A.; Xu, R.; Boyle, D. T.; Yu, Z.; Ye, Y.; Yang, Y.; Raiford, J. A.; Huang, W.; Schneider, J. R.; Cui, Y.; Bent, S. F. Electrical Resistance of the Current Collector Controls Lithium Morphology. *Nat. Commun.* **2022**, *13*, 3986 DOI: 10.1038/s41467-022-31507-w.

(123) Oyakhire, S. T.; Huang, W.; Wang, H.; Boyle, D. T.; Schneider, J. R.; de Paula, C.; Wu, Y.; Cui, Y.; Bent, S. F. Revealing and Elucidating ALD-Derived Control of Lithium Plating Microstructure. *Adv. Energy Mater.* **2020**, *10* (44), 1–11.

(124) Wu, Z.; Wang, C.; Hui, Z.; Liu, H.; Wang, S.; Yu, S.; Xing, X.; Holoubek, J.; Miao, Q.; Xin, H. L.; Liu, P. Growing Single-Crystalline

Seeds on Lithiophobic Substrates to Enable Fast-Charging Lithium-Metal Batteries. *Nat. Energy* **2023**, *8*, 340.

(125) Jana, A.; Ely, D. R.; García, R. E. Dendrite-Separator Interactions in Lithium-Based Batteries. *J. Power Sources* **2015**, *275*, 912–921.

(126) Louli, A. J.; Genovese, M.; Weber, R.; Hames, S. G.; Logan, E. R.; Dahn, J. R. Exploring the Impact of Mechanical Pressure on the Performance of Anode-Free Lithium Metal Cells. *J. Electrochem. Soc.* **2019**, *166* (8), A1291–A1299.

(127) Yin, X.; Tang, W.; Jung, I. D.; Phua, K. C.; Adams, S.; Lee, S. W.; Zheng, G. W. Insights into Morphological Evolution and Cycling Behaviour of Lithium Metal Anode under Mechanical Pressure. *Nano Energy* **2018**, *50* (August), 659–664.

(128) Lee, J. Z.; Wynn, T. A.; Schroeder, M. A.; Alvarado, J.; Wang, X.; Xu, K.; Meng, Y. S. Cryogenic Focused Ion Beam Characterization of Lithium Metal Anodes. *ACS Energy Lett.* **2019**, *4* (2), 489–493.

(129) Zachman, M. J.; Tu, Z.; Choudhury, S.; Archer, L. A.; Kourkoutis, L. F. Cryo-STEM Mapping of Solid–Liquid Interfaces and Dendrites in Lithium-Metal Batteries. *Nature* **2018**, *560* (7718), 345–349.

(130) Ye, S.; Chen, X.; Zhang, R.; Jiang, Y.; Huang, F.; Huang, H.; Yao, Y.; Jiao, S.; Chen, X.; Zhang, Q.; Yu, Y. Revisiting the Role of Physical Confinement and Chemical Regulation of 3D Hosts for Dendrite-Free Li Metal Anode. *Nano-Micro Lett.* **2022**, *14* (1), 1–17.

(131) Zhang, Y.; Qian, J.; Xu, W.; Russell, S. M.; Chen, X.; Nasibulin, E.; Bhattacharya, P.; Engelhard, M. H.; Mei, D.; Cao, R.; Ding, F.; Cresce, A. V.; Xu, K.; Zhang, J. G. Dendrite-Free Lithium Deposition with Self-Aligned Nanorod Structure. *Nano Lett.* **2014**, *14* (12), 6889–6896.

(132) Zhao, Q.; Deng, Y.; Utomo, N. W.; Zheng, J.; Biswal, P.; Yin, J.; Archer, L. A. On the Crystallography and Reversibility of Lithium Electrodeposits at Ultrahigh Capacity. *Nat. Commun.* **2021**, *12* (1), 1–10.

(133) Shi, F.; Pei, A.; Vailionis, A.; Xie, J.; Liu, B.; Zhao, J.; Gong, Y.; Cui, Y. Strong Texturing of Lithium Metal in Batteries. *Proc. Natl. Acad. Sci. U. S. A.* **2017**, *114* (46), 12138–12143.

(134) Cheng, J.-H.; Assegie, A. A.; Huang, C.-J.; Lin, M.-H.; Tripathi, A. M.; Wang, C.-C.; Tang, M.-T.; Song, Y.-F.; Su, W.-N.; Hwang, B. J. Visualization of Lithium Plating and Stripping via in Operando Transmission X-Ray Microscopy. *J. Phys. Chem. C* **2017**, *121* (14), 7761–7766.

(135) Steiger, J.; Richter, G.; Wenk, M.; Kramer, D.; Möning, R. Comparison of the Growth of Lithium Filaments and Dendrites under Different Conditions. *Electrochem. commun.* **2015**, *50*, 11–14.

(136) Steiger, J.; Kramer, D.; Möning, R. Mechanisms of Dendritic Growth Investigated by in Situ Light Microscopy during Electrodeposition and Dissolution of Lithium. *J. Power Sources* **2014**, *261*, 112–119.

(137) Vishnugopi, B. S.; Verma, A.; Mukherjee, P. P. Morphology-Safety Implications of Interfacial Evolution in Lithium Metal Anodes. *J. Phys. Chem. C* **2020**, *124* (31), 16784–16795.

(138) Thenuwara, A. C.; Shetty, P. P.; McDowell, M. T. Distinct Nanoscale Interphases and Morphology of Lithium Metal Electrodes Operating at Low Temperatures. *Nano Lett.* **2019**, *19* (12), 8664–8672.

(139) Li, Y.; Huang, W.; Li, Y.; Pei, A.; Boyle, D. T.; Cui, Y. Correlating Structure and Function of Battery Interphases at Atomic Resolution Using Cryoelectron Microscopy. *Joule* **2018**, *2* (10), 2167–2177.

(140) Hobold, G. M.; Kim, K. H.; Gallant, B. M. Beneficial vs. Inhibiting Passivation by the Native Lithium Solid Electrolyte Interphase Revealed by Electrochemical Li⁺ Exchange. *Energy Environ. Sci.* **2023**, *16*, 2247–2261.

(141) Guo, R.; Wang, D.; Zuin, L.; Gallant, B. M. Reactivity and Evolution of Ionic Phases in the Lithium Solid-Electrolyte Interphase. *ACS Energy Lett.* **2021**, *6* (3), 877–885.

(142) Wu, H.; Jia, H.; Wang, C.; Zhang, J. G.; Xu, W. Recent Progress in Understanding Solid Electrolyte Interphase on Lithium

- Metal Anodes. *Adv. Energy Mater.* **2021**, *11* (5), 2003092 DOI: [10.1002/aenm.202003092](https://doi.org/10.1002/aenm.202003092).
- (143) Zhao, Y.; Amirmaleki, M.; Sun, Q.; Zhao, C.; Codirenzi, A.; Goncharova, L. V.; Wang, C.; Adair, K.; Li, X.; Yang, X.; Zhao, F.; Li, R.; Fillette, T.; Cai, M.; Sun, X. Natural SEI-Inspired Dual-Protective Layers via Atomic/Molecular Layer Deposition for Long-Life Metallic Lithium Anode. *Matter* **2019**, *1* (5), 1215–1231.
- (144) Sun, Y.; Zhao, Y.; Wang, J.; Liang, J.; Wang, C.; Sun, Q.; Lin, X.; Adair, K. R.; Luo, J.; Wang, D.; Li, R.; Cai, M.; Sham, T. K.; Sun, X. A Novel Organic “Polyurea” Thin Film for Ultralong-Life Lithium-Metal Anodes via Molecular-Layer Deposition. *Adv. Mater.* **2019**, *31* (4), 1–9.
- (145) Chen, L.; Connell, J. G.; Nie, A.; Huang, Z.; Zavadil, K. R.; Klavetter, K. C.; Yuan, Y.; Sharifi-Asl, S.; Shahbazian-Yassar, R.; Libera, J. A.; Mane, A. U.; Elam, J. W. Lithium Metal Protected by Atomic Layer Deposition Metal Oxide for High Performance Anodes. *J. Mater. Chem. A* **2017**, *5* (24), 12297–12309.
- (146) Pearse, A. J.; Schmitt, T. E.; Fuller, E. J.; El-Gabaly, F.; Lin, C. F.; Gerasopoulos, K.; Kozen, A. C.; Talin, A. A.; Rubloff, G.; Gregorczyk, K. E. Nanoscale Solid State Batteries Enabled by Thermal Atomic Layer Deposition of a Lithium Polyphosphazene Solid State Electrolyte. *Chem. Mater.* **2017**, *29* (8), 3740–3753.
- (147) Kozen, A. C.; Lin, C.-F.; Pearse, A. J.; Schroeder, M. A.; Han, X.; Hu, L.; Lee, S.-B.; Rubloff, G. W.; Noked, M. Next-Generation Lithium Metal Anode Engineering via Atomic Layer Deposition. *ACS Nano* **2015**, *9* (6), 5884–5892.
- (148) Kazyak, E.; Chen, K. H.; Wood, K. N.; Davis, A. L.; Thompson, T.; Bielinski, A. R.; Sanchez, A. J.; Wang, X.; Wang, C.; Sakamoto, J.; Dasgupta, N. P. Atomic Layer Deposition of the Solid Electrolyte Garnet Li₇La₃Zr₂O₁₂. *Chem. Mater.* **2017**, *29* (8), 3785–3792.
- (149) Davis, A. L.; Garcia-Mendez, R.; Wood, K. N.; Kazyak, E.; Chen, K.-H.; Teeter, G.; Sakamoto, J.; Dasgupta, N. P. Electro-Chemo-Mechanical Evolution of Sulfide Solid Electrolyte/Li Metal Interfaces: Operando Analysis and ALD Interlayer Effects. *J. Mater. Chem. A* **2020**, *8* (13), 6291–6302.
- (150) Wang, C.; Zhao, Y.; Sun, Q.; Li, X.; Liu, Y.; Liang, J.; Li, X.; Lin, X.; Li, R.; Adair, K. R.; Zhang, L.; Yang, R.; Lu, S.; Sun, X. Stabilizing Interface between Li₁₀SnP₂S₁₂ and Li Metal by Molecular Layer Deposition. *Nano Energy* **2018**, *53*, 168–174.
- (151) Xu, S.; Chen, K.-H.; Dasgupta, N. P.; Siegel, J. B.; Stefanopoulou, A. G. Evolution of Dead Lithium Growth in Lithium Metal Batteries: Experimentally Validated Model of the Apparent Capacity Loss. *J. Electrochem. Soc.* **2019**, *166* (14), A3456–A3463.
- (152) McCall, C. R.; Hill, M. A.; Lillard, R. S. Crystallographic Pitting in Magnesium Single Crystals. *Corros. Eng. Sci. Technol.* **2005**, *40* (4), 337–343.
- (153) Shin, K. S.; Bian, M. Z.; Nam, N. D. Effects of Crystallographic Orientation on Corrosion Behavior of Magnesium Single Crystals. *Jom* **2012**, *64* (6), 664–670.
- (154) Wetzel, D. J.; Malone, M. A.; Haasch, R. T.; Meng, Y.; Vieker, H.; Hahn, N. T.; Götzhäuser, A.; Zuo, J. M.; Zavadil, K. R.; Gewirth, A. A.; Nuzzo, R. G. Passivation Dynamics in the Anisotropic Deposition and Stripping of Bulk Magnesium Electrodes during Electrochemical Cycling. *ACS Appl. Mater. Interfaces* **2015**, *7* (33), 18406–18414.
- (155) Jäckle, M.; Groß, A. Microscopic Properties of Lithium, Sodium, and Magnesium Battery Anode Materials Related to Possible Dendrite Growth. *J. Chem. Phys.* **2014**, *141* (17), 174710 DOI: [10.1063/1.4901055](https://doi.org/10.1063/1.4901055).
- (156) Jäckle, M.; Helmbrecht, K.; Smits, M.; Stottmeister, D.; Groß, A. Self-Diffusion Barriers: Possible Descriptors for Dendrite Growth in Batteries? *Energy Environ. Sci.* **2018**, *11* (12), 3400–3407.
- (157) Reis, F. D. A. A.; Di Caprio, D.; Taleb, A. Crossover from Compact to Branched Films in Electrodeposition with Surface Diffusion. *Phys. Rev. E* **2017**, *96* (2), 1–11.
- (158) Kinzer, B.; Davis, A. L.; Krauskopf, T.; Hartmann, H.; LePage, W. S.; Kazyak, E.; Janek, J.; Dasgupta, N. P.; Sakamoto, J. Operando Analysis of the Molten Li/LLZO Interface: Understanding How the Physical Properties of Li Affect the Critical Current Density. *Matter* **2021**, *4* (6), 1947–1961.
- (159) Zhang, X.; Wang, Q. J.; Harrison, K. L.; Jungjohann, K.; Boyce, B. L.; Roberts, S. A.; Attia, P. M.; Harris, S. J. Rethinking How External Pressure Can Suppress Dendrites in Lithium Metal Batteries. *J. Electrochem. Soc.* **2019**, *166* (15), A3639–A3652.
- (160) Lee, Y. G.; Fujiki, S.; Jung, C.; Suzuki, N.; Yashiro, N.; Omoda, R.; Ko, D. S.; Shiratsuchi, T.; Sugimoto, T.; Ryu, S.; Ku, J. H.; Watanabe, T.; Park, Y.; Aihara, Y.; Im, D.; Han, I. T. High-Energy Long-Cycling All-Solid-State Lithium Metal Batteries Enabled by Silver–Carbon Composite Anodes. *Nat. Energy* **2020**, *5* (4), 299–308.
- (161) Hatzell, K. B.; Chen, X. C.; Cobb, C. L.; Dasgupta, N. P.; Dixit, M. B.; Marbella, L. E.; McDowell, M. T.; Mukherjee, P. P.; Verma, A.; Viswanathan, V.; Westover, A. S.; Zeier, W. G. Challenges in Lithium Metal Anodes for Solid-State Batteries. *ACS Energy Lett.* **2020**, *5* (3), 922–934.
- (162) Krauskopf, T.; Richter, F. H.; Zeier, W. G.; Janek, J. Physicochemical Concepts of the Lithium Metal Anode in Solid-State Batteries. *Chem. Rev.* **2020**, *120* (15), 7745–7794.
- (163) Albertus, P.; Anandan, V.; Ban, C.; Balsara, N.; Belharouak, I.; Buettner-Garrett, J.; Chen, Z.; Daniel, C.; Doeff, M.; Dudney, N. J.; Dunn, B.; Harris, S. J.; Herle, S.; Herbert, E.; Kalnaus, S.; Libera, J. A.; Lu, D.; Martin, S.; McCloskey, B. D.; McDowell, M. T.; Meng, Y. S.; Nanda, J.; Sakamoto, J.; Self, E. C.; Tepavcevic, S.; Wachsman, E.; Wang, C.; Westover, A. S.; Xiao, J.; Yersak, T. Challenges for and Pathways toward Li-Metal-Based All-Solid-State Batteries. *ACS Energy Lett.* **2021**, *6* (4), 1399–1404.
- (164) Liu, J.; Yuan, H.; Liu, H.; Zhao, C. Z.; Lu, Y.; Cheng, X. B.; Huang, J. Q.; Zhang, Q. Unlocking the Failure Mechanism of Solid State Lithium Metal Batteries. *Adv. Energy Mater.* **2022**, *12* (4), 1–19.
- (165) Wang, C.; Deng, T.; Fan, X.; Zheng, M.; Yu, R.; Lu, Q.; Duan, H.; Huang, H.; Wang, C.; Sun, X. Identifying Soft Breakdown in All-Solid-State Lithium Battery. *Joule* **2022**, *6* (8), 1770–1781.
- (166) Li, B.; Chao, Y.; Li, M.; Xiao, Y.; Li, R.; Yang, K.; Cui, X.; Xu, G.; Li, L.; Yang, C.; Yu, Y.; Wilkinson, D. P.; Zhang, J. A Review of Solid Electrolyte Interphase (SEI) and Dendrite Formation in Lithium Batteries; Springer Nature: Singapore, 2023; Vol. 6 DOI: [10.1007/s41918-022-00147-5](https://doi.org/10.1007/s41918-022-00147-5).
- (167) Lin, D.; Liu, Y.; Li, Y.; Pei, A.; Xie, J.; Huang, W.; Cui, Y. Fast Galvanic Lithium Corrosion Involving a Kirkendall-Type Mechanism. *Nat. Chem.* **2019**, *11* (4), 382–389.
- (168) Kolesnikov, A.; Kolek, M.; Dohmann, J. F.; Horsthemke, F.; Börner, M.; Bieker, P.; Winter, M.; Stan, M. C. Galvanic Corrosion of Lithium-Powder-Based Electrodes. *Adv. Energy Mater.* **2020**, *10* (15), 1–9.
- (169) Boyle, D. T.; Huang, W.; Wang, H.; Li, Y.; Chen, H.; Yu, Z.; Zhang, W.; Bao, Z.; Cui, Y. Corrosion of Lithium Metal Anodes during Calendar Ageing and Its Microscopic Origins. *Nat. Energy* **2021**, *6* (5), 487–494.
- (170) Kwon, B.; Lee, J.; Kim, H.; Kim, D. M.; Park, K.; Jo, S.; Lee, K. T. Janus Behaviour of LiFSI- And LiPF₆-Based Electrolytes for Li Metal Batteries: Chemical Corrosion: Versus Galvanic Corrosion. *J. Mater. Chem. A* **2021**, *9* (44), 24993–25003.
- (171) Dohmann, J. F.; Horsthemke, F.; KüPers, V.; Bloch, S.; Preibisch, Y.; Kolesnikov, A.; Kolek, M.; Stan, M. C.; Winter, M.; Bieker, P. Galvanic Couples in Ionic Liquid-Based Electrolyte Systems for Lithium Metal Batteries—An Overlooked Cause of Galvanic Corrosion? *Adv. Energy Mater.* **2021**, *11* (24), 2101021 DOI: [10.1002/aenm.202101021](https://doi.org/10.1002/aenm.202101021).
- (172) Mehdi, B. L.; Qian, J.; Nasybulin, E.; Park, C.; Welch, D. A.; Faller, R.; Mehta, H.; Henderson, W. A.; Xu, W.; Wang, C. M.; Evans, J. E.; Liu, J.; Zhang, J. G.; Mueller, K. T.; Browning, N. D. Observation and Quantification of Nanoscale Processes in Lithium Batteries by Operando Electrochemical (S)TEM. *Nano Lett.* **2015**, *15* (3), 2168–2173.
- (173) Adams, B. D.; Zheng, J.; Ren, X.; Xu, W.; Zhang, J. G. Accurate Determination of Coulombic Efficiency for Lithium Metal

Anodes and Lithium Metal Batteries. *Adv. Energy Mater.* **2018**, 8 (7), 1–11.

(174) Parejiya, A.; Amin, R.; Essehli, R.; Wood, D. L.; Belharouak, I. Electrochemical Healing of Dendrites in Garnet-Based Solid Electrolytes. *ACS Energy Lett.* **2020**, 5 (11), 3368–3373.

(175) Liu, H.; Cheng, X. B.; Xu, R.; Zhang, X. Q.; Yan, C.; Huang, J. Q.; Zhang, Q. Plating/Stripping Behavior of Actual Lithium Metal Anode. *Adv. Energy Mater.* **2019**, 9 (44), 1–7.

(176) Verma, A.; Kawakami, H.; Wada, H.; Hirowatari, A.; Ikeda, N.; Mizuno, Y.; Kotaka, T.; Aotani, K.; Tabuchi, Y.; Mukherjee, P. P. Microstructure and Pressure-Driven Electrodeposition Stability in Solid-State Batteries. *Cell Reports Phys. Sci.* **2021**, 2 (1), No. 100301.

(177) Kasemchainan, J.; Zekoll, S.; Spencer Jolly, D.; Ning, Z.; Hartley, G. O.; Marrow, J.; Bruce, P. G. Critical Stripping Current Leads to Dendrite Formation on Plating in Lithium Anode Solid Electrolyte Cells. *Nat. Mater.* **2019**, 18 (10), 1105–1111.

(178) Lewis, J. A.; Cortes, F. J. Q.; Liu, Y.; Miers, J. C.; Verma, A.; Vishnugopi, B. S.; Tippens, J.; Prakash, D.; Marchese, T. S.; Han, S. Y.; Lee, C.; Shetty, P. P.; Lee, H. W.; Shevchenko, P.; De Carlo, F.; Saldana, C.; Mukherjee, P. P.; McDowell, M. T. Linking Void and Interphase Evolution to Electrochemistry in Solid-State Batteries Using Operando X-Ray Tomography. *Nat. Mater.* **2021**, 20 (4), 503–510.

(179) Lee, K.; Kazyak, E.; Wang, M. J.; Dasgupta, N. P.; Sakamoto, J. Analyzing Void Formation and Rewetting of Thin In Situ-Formed Li Anodes on LLZO. *Joule* **2022**, 6 (11), 2547–2565.

(180) Roy, U.; Fleck, N. A.; Deshpande, V. S. An Assessment of a Mechanism for Void Growth in Li Anodes. *Extrem. Mech. Lett.* **2021**, 46, No. 101307.